



Lie Group Spectral Variational Integrators

James Hall¹ · Melvin Leok¹

Received: 14 February 2014 / Revised: 9 July 2015 / Accepted: 17 August 2015 /
Published online: 11 November 2015
© SFoCM 2015

Abstract We present a new class of high-order variational integrators on Lie groups. We show that these integrators are symplectic and momentum-preserving, can be constructed to be of arbitrarily high order, or can be made to converge geometrically. Furthermore, these methods are capable of taking very large time-steps. We demonstrate the construction of one such variational integrator for the rigid body and discuss how this construction could be generalized to other related Lie group problems. We close with several numerical examples which demonstrate our claims and discuss further extensions of our work.

Keywords Symplectic integrators · Variational integrators · Lie group integrators · Geometric numerical integration

Mathematics Subject Classification 37M15 · 65M70 · 65P10 · 70G75 · 70H25

1 Introduction

There is a deep and elegant geometric structure underlying the dynamics of many mechanical systems. Conserved quantities, such as the energy, momentum, and symplectic form offer insight into this structure, and through this, we obtain an under-

Communicated by Arieh Iserles.

✉ Melvin Leok
mleok@math.ucsd.edu

James Hall
j9hall@math.ucsd.edu

¹ Department of Mathematics, University of California, San Diego, 9500 Gilman Drive #0112, La Jolla, CA 92093-0112, USA

standing of the behavior of these systems that goes beyond what is conventionally available. Conservation laws reveal much about the stability and long term behavior of a system and can even characterize the entire dynamics of a system when a sufficient number of them exist. Hence, there has been much recent interest in the field of geometric mechanics, which seeks to understand this structure using differential geometric and symmetry techniques.

From this geometric mechanics framework, it is possible to formulate numerical methods which respect much of the geometry of mechanical systems. There are a variety of approaches for constructing such methods, often known as *structure-preserving methods*, including projection methods, splitting methods, symplectic Runge–Kutta methods, and B-series expansion methods. An extensive introduction can be found in Hairer et al. [12]. One of the powerful frameworks, discrete mechanics, approaches the construction of numerical methods by developing much of the theory of geometric mechanics from a discrete standpoint. This approach has proven highly effective for constructing methods for problems in Hamiltonian and Lagrangian mechanics, specifically because these type of problems arise from a variational principle. Methods that make use of a variational principle and the framework of discrete mechanics are referred to as *variational integrators*, and they have many favorable geometric properties, including conservation of the symplectic form and momentum. A comprehensive survey of discrete mechanics and variational integrators can be found in Marsden and West [28].

A further advantage of variational integrators is that it is often straightforward to analyze the error of these methods. This has led to the development of high-order variational integrators, which can be constructed so that they converge very quickly. In Hall and Leok [13], such integrators for vector space problems were presented and analyzed. It was shown that such integrators can be arbitrarily high order or even exhibit geometric convergence. Furthermore, these integrators are capable of taking extremely large time-steps, and by using them, it is easy to reconstruct highly accurate continuous approximations to the dynamics of the system of interest.

In this paper, we present an extension of that work to Lie group methods. Lie group methods are of particular interest in science and engineering applications. It can be shown that many problems of interest, from the dynamics of rigid bodies to the behavior of incompressible fluids, evolve in Lie groups. Furthermore, if a traditional numerical method is applied to a problem with dynamics in a Lie group, the approximate solution will typically depart from the Lie group, destroying a critical structural property of the solution. Our work gives a general framework for constructing methods which will always evolve in the Lie group and which will share many of the desirable properties of the vector space type methods. Specifically, we will be able to construct methods of arbitrarily high order and with geometric convergence, and we will be able to reconstruct high-quality continuous approximations from these methods.

Lie group methods have a rich history and remain the subject of significant interest. An extensive introduction can be found in Iserles et al. [14], which provides an excellent exposition of both the motivation for Lie group methods and many of the techniques used on Lie groups. Likewise, Celledoni and Owren [8] provide a very helpful general introduction to Lie group methods for the rigid body, which is a prototypical example of an interesting Lie group problem. The free rigid body is an example

of a Lie–Poisson system, which is obtained by symmetry reduction. Lie–Poisson integrators were discussed in Zhong and Marsden [40], and further developed in Channell and Scovel [9]. A more recent perspective can be found in McLachlan and Scovel [34], and an approach based on equivariant constraints was developed in Marsden et al. [33]. A discrete theory of reduction in the Euler–Poincaré and Lie–Poisson setting was introduced in Marsden et al. [30, 31], and for the case of abelian Routh reduction in Jalnapurkar et al. [15]. Additionally, the free rigid body is completely integrable, and the question of integrable discretizations was studied in Moser and Veselov [35] and Bobenko and Suris [1].

In this paper, we provide a thorough example of the construction of our method for the rigid body, as this approach can easily be extended to other interesting problems. Partitioned Runge–Kutta methods were used by Jay [16, 17] to construct high-order structure-preserving integrators that preserved holonomic constraints. Bou-Rabee and Marsden [3] combined Lie group methods with the discrete Hamilton–Pontryagin principle to obtain a class of high-order symplectic Lie group integrators, in particular, the variational Runge–Kutta–Munthe-Kaas and variational Crouch–Grossman integrators, and Bogfjellmo and Marthinsen [2] developed the order theory in the context of variational error analysis for these methods. Burnett et al. [7] introduced a generalization of high-order Lie group discretizations to higher-order variational problems, and applied this to interpolation in $SO(3)$.

Galerkin variational integrators were proposed in Marsden and West [28], and expanded on by Leok [23, Chapter 5]. The concept of a Galerkin Lie group integrator was proposed in Leok [23, Chapter 5] and expanded in Leok and Shingel [24]. Our work expands upon this by generalizing both the diffeomorphisms used to construct the natural charts and the approximation spaces used to construct the curve on the Lie group, and establishing convergence results and properties of both the discrete solution and the continuous approximation.

1.1 Discrete Mechanics

Since we are working from the perspective of discrete mechanics, we will take a moment to review the fundamentals of the theory here. This will only be a brief summary, and extensive exposition of the theory can be found in Marsden and West [28].

Consider a configuration manifold, Q , which describes the configuration of a mechanical system at a given point in time. In discrete mechanics, the fundamental object is the *discrete Lagrangian*, $L_d : Q \times Q \times \mathbb{R} \rightarrow \mathbb{R}$. The discrete Lagrangian can be viewed as an approximation to the *exact discrete Lagrangian* L_d^E , where the L_d^E is defined to be the action of the Lagrangian on the solution of the Euler–Lagrange equations over a short time interval:

$$L_d(q_0, q_1, h) \approx L_d^E(q_0, q_1, h) = \underset{\substack{q \in C^2([0, h], Q) \\ q(0)=q_0, q(h)=q_1}}{\text{ext}} \int_0^h L(q, \dot{q}) dt.$$

The discrete Lagrangian gives rise to a discrete action sum, which can be viewed as an approximation to the action over a long time interval:

$$\mathbb{S}(\{q_k\}_{k=1}^n) = \sum_{k=0}^{n-1} L_d(q_k, q_{k+1}, h) \approx \int_{t_0}^{t_n} L(q, \dot{q}) dt,$$

and requiring stationarity of this discrete action sum subject to fixed endpoint conditions q_0, q_n , gives rise to the *discrete Euler–Lagrange equations*:

$$D_1 L_d(q_k, q_{k+1}, h) + D_2 L_d(q_{k-1}, q_k, h) = 0, \tag{1}$$

where D_i denotes partial differentiation of a function with respect to the i -th argument. Given a point (q_{k-1}, q_k) , these equations implicitly define an update map $F_{L_d} : (q_{k-1}, q_k) \rightarrow (q_k, q_{k+1})$, which approximates the solution of the Euler–Lagrange equations for the continuous system. In particular, q_k should be viewed as an approximation of the continuous solution q of the Euler–Lagrange equation at time $t_k = kh$, i.e., $q_k \approx q(kh)$. A numerical method which uses the update map F_{L_d} to construct numerical solutions to ODEs is referred to as a *variational integrator*.

Since variational integrators are examples of symplectic integrators, and symplectic integrators are often used with fixed time-steps in order to achieve bounded energy errors for exponentially long times, we will often suppress the third argument h in the discrete Lagrangian for notational simplicity, and consider it as a function $L_d : Q \times Q \rightarrow \mathbb{R}$. Which of these we are referring to should be clear from the context.

The power of discrete mechanics is derived from the discrete variational structure. Since the update map F_{L_d} is induced from a discrete analogue of the variational principle, much of the geometric structure from continuous mechanics can be extended to discrete mechanics. The discrete Lagrangian gives rise to *discrete Legendre Transforms* $\mathbb{F}L^\pm : Q \times Q \rightarrow T^*Q$:

$$\begin{aligned} \mathbb{F}L_d^+(q_k, q_{k+1}) &= (q_{k+1}, D_2 L_d(q_k, q_{k+1})), \\ \mathbb{F}L_d^-(q_k, q_{k+1}) &= (q_k, -D_1 L_d(q_k, q_{k+1})), \end{aligned}$$

which lead to the extension of other classical geometric structures. It is important to note that, while there are two different discrete Legendre transforms, (1) guarantees that $\mathbb{F}L_d^-(q_k, q_{k+1}) = \mathbb{F}L_d^+(q_{k-1}, q_k)$, and thus they can be used interchangeably when defining the discrete geometric structure. By their construction, variational integrators induce a discrete symplectic form by pullback, i.e., $\Omega_{L_d} = (\mathbb{F}^\pm L_d)^* \Omega$ which is conserved by the update map $F_{L_d}^* \Omega_{L_d} = \Omega_{L_d}$, and a discrete analogue of Noether’s Theorem, which states that if a discrete Lagrangian is invariant under a diagonal group action on (q_k, q_{k+1}) , it induces a discrete momentum map $J_{L_d} = (\mathbb{F}L_d^\pm)^* J$, which is preserved under the update map: $F_{L_d}^* J_{L_d} = J_{L_d}$. The existence of these discrete geometric conservation laws gives a systematic framework to construct powerful numerical methods which preserve structure.

The discrete Legendre transforms also allow us to define an update map on phase space $\tilde{F}_{L_d} : T^*Q \rightarrow T^*Q$,

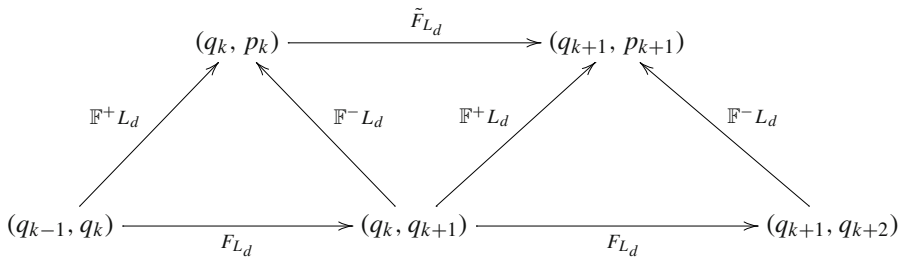
$$\tilde{F}_{L_d}(q_k, p_k) = (q_{k+1}, p_{k+1}),$$

which is given by

$$\tilde{F}_{L_d}(q_k, p_k) = \mathbb{F}^+ L_d \left((\mathbb{F}^- L_d)^{-1}(q_k, p_k) \right),$$

known as the Hamiltonian flow map. As long as the discrete Lagrangian is sufficiently smooth, the Hamiltonian flow map and the Lagrangian flow map are compatible, and the geometric structure of discrete flow can be understood from either perspective, just as in the continuous theory.

The following commutative diagram illustrates the relationship between the discrete Legendre transforms, the Lagrangian flow map, the Hamiltonian flow map, and the discrete Lagrangian.



A further consequence of the discrete mechanics framework is that it provides a natural mechanism for analyzing the order of accuracy of a variational integrator. Specifically, it can be shown that the variational integrator induced by the exact discrete Lagrangian produces an exact sampling of the true flow. Based on this, we have the following theorem which is critical for the error analysis of variational integrators:

Theorem 1.1 Variational Order Analysis (Theorem 2.3.1 of Marsden and West [28])
If a discrete Lagrangian L_d approximates the exact discrete Lagrangian L_d^E to order p , i.e., $L_d(q_0, q_1, h) = L_d^E(q_0, q_1, h) + \mathcal{O}(h^{p+1})$, then the variational integrator induced by L_d is order p accurate.

This theorem allows for greatly simplified *a priori* error estimates of variational integrators, and is a fundamental tool for the development and analysis of high-order variational integrators. A refinement of this result can found in Patrick and Cuell [37].

2 Construction

2.1 General Galerkin Variational Integrators

Lie group Galerkin variational integrators are an extension of Galerkin variational integrators to Lie groups. As such, we will briefly review the construction of general Galerkin variational integrators.

The driving idea behind Galerkin variational integrators is to approach the construction of a discrete Lagrangian as the approximation of a variational problem. We know from discrete mechanics that the exact discrete Lagrangian $L_d^E : Q \times Q \times \mathbb{R} \rightarrow \mathbb{R}$,

$$L_d^E(q_0, q_1, h) = \underset{\substack{q \in C^2([0, h], Q) \\ q(0)=q_0, q(h)=q_1}}{\text{ext}} \int_0^h L(q, \dot{q}) dt,$$

induces a variational integrator that produces an exact sampling of the true flow, and the accuracy with which a variational integrator approximates the true solution is the same as the accuracy to which the discrete Lagrangian used to construct it approximates the exact discrete Lagrangian. Hence, to construct a highly accurate discrete Lagrangian, we construct a discrete approximation

$$\begin{aligned} L_d^G(q_0, q_1, h) &= \underset{\substack{q_n \in \mathbb{M}^n([0, h], Q) \\ q_n(0)=q_0, q_n(h)=q_1}}{\text{ext}} h \sum_{j=1}^m b_j L(q_n(c_j h), \dot{q}_n(c_j h)) \\ &\approx \underset{\substack{q \in C^2([0, h], Q) \\ q(0)=q_0, q(h)=q_1}}{\text{ext}} \int_0^h L(q, \dot{q}) dt \end{aligned}$$

by replacing the function space $C^2([0, h], Q)$ with a finite-dimensional subspace $\mathbb{M}^n([0, h], Q) \subset C^2([0, h], Q)$ and the integral with a quadrature rule, $h \sum_{j=1}^m b_j f(c_j h) \approx \int_0^h f dt$ (where $q_n(t)$ is a curve through the configuration space Q that is also an element of the finite-dimensional approximation space). Finding the extremizer of the discrete action is a tractable numerical problem, and by computing this extremizer we can construct the variational integrator that results from the discrete Lagrangian. Because this approach of replacing the function space $C^2([0, h], Q)$ with a finite-dimensional subspace is inspired by Galerkin methods for partial differential equations, we refer to variational integrators constructed in this way as *Galerkin variational integrators*.

In Hall and Leok [13], we studied Galerkin variational integrators on linear spaces. Specifically, we obtained several significant results, including that Galerkin variational integrators for linear spaces can be constructed to be of arbitrarily high order, and that by enriching the function space $\mathbb{M}^n([0, h], Q)$, as opposed to shortening the time-step h , we can construct variational integrators that converge geometrically. Furthermore, we established that it is easy to recover a continuous approximation to the trajectory over the time interval $[0, h]$, and that the convergence of this continuous approximation is related to the rate of convergence of the variational integrator. Finally, we established an error bound on Noether quantities evaluated on this continuous approximation which is independent of the number of steps taken.

2.2 Lie Group Galerkin Variational Integrators

The construction and analysis in Hall and Leok [13] relied on the linear structure of the spaces involved. At their heart, Galerkin variational integrators make use of a Galerkin curve

$$\tilde{q}_n(t) = \sum_{i=0}^n q^i \phi_i(t)$$

for some set of points $\{q^i\}_{i=0}^n \subset Q$ and basis functions $\{\phi_i\}_{i=0}^n \subset C^2([0, h], \mathbb{R})$. While for linear spaces, $\tilde{q}_n(t) \in Q$ for any choice of t , in nonlinear spaces this will not be the case. However, when Q is a Lie group, it is possible to extend this construction in a way that keeps the curve $\tilde{q}_n(t)$ in Q .

2.2.1 Natural Charts

To generalize Galerkin variational integrators to Lie groups, we will make use of the linear nature of the Lie algebra associated with the Lie group. Specifically, given a Lie group G and its associated Lie algebra \mathfrak{g} , we choose a local diffeomorphism $\Phi : \mathfrak{g} \rightarrow G$. Then, given a set of points in the Lie group $\{g_i\}_{i=1}^n \subset G$ and a set of associated interpolation times t_i , we can construct an interpolating curve $g : G^n \times \mathbb{R} \rightarrow G$ such that $g(\{g_i\}_{i=1}^n, t_i) = g_i$, given by

$$g(\{g_i\}_{i=0}^n, t) = L_{g_0} \Phi \left(\sum_{i=0}^n \Phi^{-1} \left(L_{g_0^{-1}} g_i \right) \phi_i(t) \right),$$

where L_g is the left group action of g and $\phi_i(t)$ is the Lagrange interpolation polynomial for t_i . This type of curve is *Lie group equivariant*, that is, $g(\{L_{\hat{g}} g_i\}_{i=1}^n, t) = L_{\hat{g}} g(\{g_i\}_{i=0=1}^n, t)$ for any $\hat{g} \in G$, as we shall show in the following lemma.

Lemma 2.1 *The curve $g(\{g_i\}_{i=0}^n, t)$ is Lie group equivariant.*

Proof The proof is a direct calculation.

$$\begin{aligned} g(\{L_{\hat{g}} g_i\}, t) &= L_{L_{\hat{g}} g_0} \Phi \left(\sum_{i=0}^n \Phi^{-1} \left(L_{(L_{\hat{g}} g_0)^{-1}} L_{\hat{g}} g_i \right) \phi_i(t) \right) \\ &= L_{\hat{g}} L_{g_0} \Phi \left(\sum_{i=0}^n \Phi^{-1} \left(L_{g_0^{-1}} L_{\hat{g}^{-1}} L_{\hat{g}} g_i \right) \phi_i(t) \right) \\ &= L_{\hat{g}} L_{g_0} \Phi \left(\sum_{i=0}^n \Phi^{-1} \left(L_{g_0^{-1}} g_i \right) \phi_i(t) \right) \\ &= L_{\hat{g}} g(\{g_i\}_{i=0}^n, t). \end{aligned}$$

□

This property will be important for ensuring that the Lie group Galerkin discrete Lagrangian inherits the symmetries of the continuous Lagrangian; these inherited symmetries give rise to the structure-preserving properties of the resulting variational integrator.

Throughout this paper, we will consider the function spaces composed of curves of this form. We note that $\Phi^{-1}(L_{g_0^{-1}} g_i) \in \mathfrak{g}$, and for any $\xi \in \mathfrak{g}$, $L_{g_0} \Phi(\xi) \in G$, so we can construct interpolation curves on the group in terms of interpolation curves in the Lie algebra. In light of this, we define

$$\mathbb{GM}^n (g_0 \times [0, h], G) := \left\{ g \left(\left\{ \xi^i \right\}_{i=0}^n, t \right) \mid g \left(\left\{ \xi^i \right\}_{i=1}^n, t \right) = L_{g_0} \Phi \left(\sum_{i=1}^n \xi^i \phi_i (t) \right), \xi^i \in \mathfrak{g} \right\}$$

where $\{\phi_i (t)\}_{i=0}^n$ forms the basis for a finite-dimensional approximation space in \mathbb{R} , for example, Lagrange interpolation polynomials, which is what we will use in our explicit construction in Sect. 4 and numerical examples in Sect. 5. We refer to the space of finite-dimensional curves in the Lie algebra as

$$\mathbb{M}^n ([0, h], \mathfrak{g}) = \left\{ \xi (t) \mid \xi (t) = \sum_{i=1}^n \xi^i \phi_i (t), \xi^i \in \mathfrak{g}, \phi_i : [0, h] \rightarrow \mathbb{R} \right\}.$$

Because we are identifying every point in a neighborhood of the Lie group with a point in the Lie algebra, which is a vector space, it is natural to think of this construction as choosing a set of coordinates for a neighborhood in the Lie group. Thus, we can consider this construction as choosing a chart for a neighborhood of the Lie group, and because it makes use of the “natural” relationship between the Lie group G , its Lie algebra \mathfrak{g} , and the tangent space of the Lie group TG , we call the function $\varphi_{g_0} : G \rightarrow \mathfrak{g}, \varphi_{g_0} (\cdot) = \Phi^{-1} (L_{g_0}^{-1} (\cdot))$ a “natural chart.”

2.2.2 Discrete Lagrangian

Now that we have introduced a Lie group approximation space, we can define a compatible discrete Lagrangian for Lie group problems. We take a similar approach to the construction for vector spaces; we construct an approximation to the action of the Lagrangian over $[0, h]$ by replacing $C^2 ([0, h], G)$ with a finite-dimensional approximation space and the integral with a quadrature rule, and then compute its extremizer. Specifically, given a Lagrangian on the tangent space of a Lie group $L : TG \rightarrow \mathbb{R}$, the associated Lie group Galerkin discrete Lagrangian is defined to be:

$$L_d (g_k, g_{k+1}, h) = \underset{\substack{g_n \in \mathbb{GM}^n (g_k \times [0, h], G) \\ g_n (0) = g_k, g_n (h) = g_{k+1}}}{\text{ext}} h \sum_{j=1}^m b_j L (g_n (c_j h), \dot{g}_n (c_j h)).$$

2.2.3 Internal Stage Discrete Euler–Lagrange Equations

This discrete Lagrangian involves solving an optimization problem, namely: find $\tilde{g}_n (t) \in \mathbb{GM}^n (g_k \times [0, h], G)$ such that $\tilde{g}_n (0) = g_k, \tilde{g}_n (h) = g_{k+1}$, and

$$h \sum_{j=1}^m b_j L (\tilde{g}_n (c_j h), \dot{\tilde{g}}_n (c_j h)) = \underset{\substack{g_n \in \mathbb{GM}^n (g_k \times [0, h], G) \\ g_n (0) = g_k, g_n (h) = g_{k+1}}}{\text{ext}} h \sum_{j=1}^m b_j L (g_n (c_j h), \dot{g}_n (c_j h)). \tag{2}$$

While this problem can be solved using standard methods of numerical optimization, it is also possible to reduce it to a root-finding problem. Since each curve $\tilde{g}_n(t) \in \mathbb{GM}^n(g_0 \times [0, h], G)$ is parametrized by a finite number of Lie algebra points $\{\xi^i\}_{i=1}^n$, by taking discrete variations of the discrete Lagrangian with respect to these points, we can derive stationarity conditions for the extremizer. Specifically, if we denote

$$\xi(t) = \sum_{i=1}^n \xi^i \phi_i(t)$$

and take $\mathbf{D}_p f$ to denote the differential of a map f at the point p , with the short hand of

$$\begin{aligned} \mathbf{D}_1 L(x, y) &= \mathbf{D}_x L(x), \text{ considering the Lagrangian as just} \\ &\text{a function of its first argument} \\ \mathbf{D}_2 L(x, y) &= \mathbf{D}_y L(y), \text{ considering the Lagrangian as just} \\ &\text{a function of its second argument} \end{aligned}$$

then a straightforward computation reveals the stationarity condition:

$$\begin{aligned} h \sum_{j=1}^m b_j &\left(\mathbf{D}_1 L \circ \mathbf{D}_{\Phi(\xi(c_j h))} L_{g_k} \circ \mathbf{D}_{\xi(c_j h)} \Phi \circ \left(\sum_{i=1}^n \mathbf{D}_{\xi^i} \xi(c_j h) \cdot \delta \xi^i \right) \right. \\ &+ \mathbf{D}_2 L \circ \mathbf{D}_{\left(\Phi \circ \xi(c_j h), \mathbf{D}_{\dot{\xi}(c_j h)} \Phi \circ \dot{\xi}(c_j h) \right)} \mathbf{D}_{\Phi \circ \xi(c_j h)} L_{g_k} \circ \mathbf{D}_{\left(\xi(c_j h), \dot{\xi}(c_j h) \right)} \Phi \\ &\left. \circ \left(\sum_{i=1}^n \mathbf{D}_{\xi^i} \dot{\xi}(c_j h) \cdot \delta \xi^i \right) \right) = 0 \end{aligned}$$

for arbitrary $\{\delta \xi^i\}_{i=1}^n$. Using standard calculus of variations arguments, this reduces to

$$\begin{aligned} h \sum_{j=1}^m b_j &\left(\mathbf{D}_1 L \circ \mathbf{D}_{\Phi(\xi(c_j h))} L_{g_k} \circ \mathbf{D}_{\xi(c_j h)} \Phi \circ \mathbf{D}_{\xi^i} \xi(c_j h) \cdot \delta \xi^i \right. \\ &+ \mathbf{D}_2 L \circ \mathbf{D}_{\left(\Phi \circ \xi(c_j h), \mathbf{D}_{\dot{\xi}(c_j h)} \Phi \circ \dot{\xi}(c_j h) \right)} \mathbf{D}_{\Phi \circ \xi(c_j h)} L_{g_k} \\ &\left. \circ \mathbf{D}_{\left(\xi(c_j h), \dot{\xi}(c_j h) \right)} \Phi \circ \mathbf{D}_{\xi^i} \dot{\xi}(c_j h) \cdot \delta \xi^i \right) = 0 \end{aligned}$$

for $i = 2, \dots, n - 1$ (note that the sum of the Lie algebra elements has disappeared). Now using the linearity of one-forms, we can collect terms to further simplify this expression to

$$\begin{aligned}
 & h \sum_{j=1}^m b_j \left(\left[\mathbf{D}_1 L \circ \mathbf{D}_{\Phi(\xi(c_j h))} L_{g_k} \circ \mathbf{D}_{\xi(c_j h)} \Phi \circ \mathbf{D}_{\xi^i \xi}(c_j h) \right. \right. \\
 & \quad + \mathbf{D}_2 L \circ \mathbf{D}_{\left(\Phi \circ \xi(c_j h), \mathbf{D}_{\xi(c_j h)} \Phi \circ \xi(c_j h) \right)} \mathbf{D}_{\Phi \circ \xi(c_j h)} L_{g_k} \\
 & \quad \left. \left. \circ \mathbf{D}_{\left(\xi(c_j h), \dot{\xi}(c_j h) \right)} \Phi \circ \mathbf{D}_{\xi^i \dot{\xi}}(c_j h) \right] \cdot \delta \xi^i \right) = 0
 \end{aligned}$$

for $i = 2, \dots, n - 1$. Since $\delta \xi^i$ is arbitrary, this implies that

$$\begin{aligned}
 & h \sum_{j=1}^m b_j \left(\mathbf{D}_1 L \circ \mathbf{D}_{\Phi(\xi(c_j h))} L_{g_k} \circ \mathbf{D}_{\xi(c_j h)} \Phi \circ \mathbf{D}_{\xi^i \xi}(c_j h) \cdot \right. \\
 & \quad + \mathbf{D}_2 L \circ \mathbf{D}_{\left(\Phi \circ \xi(c_j h), \mathbf{D}_{\xi(c_j h)} \Phi \circ \dot{\xi}(c_j h) \right)} \mathbf{D}_{\Phi \circ \xi(c_j h)} L_{g_k} \\
 & \quad \left. \circ \mathbf{D}_{\left(\xi(c_j h), \dot{\xi}(c_j h) \right)} \Phi \circ \mathbf{D}_{\xi^i \dot{\xi}}(c_j h) \right) = 0 \tag{3}
 \end{aligned}$$

for $i = 2, \dots, n - 1$. These equations, which we shall refer to as the *internal stage discrete Euler–Lagrange equations*, combined with the standard momentum matching condition,

$$D_2 L_d(g_{k-1}, g_k) + D_1 L_d(g_k, g_{k+1}) = 0, \tag{4}$$

which we will discuss in more detail in the Sect. 2.2.4, can be easily solved with an iterative nonlinear equation solver. The result is a curve $\tilde{g}_n(t)$ which satisfies condition (2). The next step of the one-step map is given by $\tilde{g}_n(h) = g_{k+1}$, which gives the variational integrator.

It should be noted that while the internal stage discrete Euler–Lagrange equations can be computed by deriving all of the various differentials in the chosen coordinates, it is often much simpler to form the discrete action

$$\mathbb{S}_d \left(\left\{ \xi^i \right\}_{i=1}^n \right) = h \sum_{j=1}^m b_j L \left(L_{g_k} \Phi \left(\sum_{i=1}^n \xi^i \phi_i(c_j h) \right), \frac{d}{dt} \left(L_{g_k} \Phi \left(\sum_{i=1}^n \xi^i \phi_i(c_j h) \right) \right) \right)$$

explicitly and then compute the stationarity conditions directly in coordinates, rather than a step-by-step computation of the different maps in (3). This is the approach we take when deriving the integrator for the rigid body in Sect. 4, and it appears to be the much simpler approach in this case. However, the two approaches are equivalent, so if done carefully either will suffice to give the internal stage Euler–Lagrange equations.

2.2.4 Momentum Matching Condition

A difficulty in the derivation of the discrete Euler–Lagrange equations is the computation of the discrete momentum terms

$$p_{k,k+1}^- = -D_1 L_d(g_k, g_{k+1})$$

$$p_{k-1,k}^+ = D_2 L_d (g_{k-1}, g_k)$$

which are used in the discrete Euler–Lagrange equations (4),

$$D_1 L_d (g_k, g_{k+1}) + D_2 L_d (g_{k-1}, g_k) = 0$$

or

$$p_{k-1,k}^+ = p_{k,k+1}^-.$$

The difficulty arises because the discrete Lagrangian makes use of a local left trivialization. Through the local charts, we reduce the discrete Lagrangian to a function of algebra elements, and because the corresponding group elements are recovered through a complicated computation, working with the group elements directly to compute the discrete Euler–Lagrange equations is difficult. Because of this, to compute the discrete Euler–Lagrange equations, it is more natural to think of the discrete Lagrangian as a function of two Lie algebra elements. If we define a discrete Lagrangian on the Lie algebra $\hat{L}_d : \mathfrak{g} \times \mathfrak{g} \times h \rightarrow \mathbb{R}$ as

$$\begin{aligned} \hat{L}_d (\xi_k, \xi_{k+1}, h) = & \text{ext}_{g_n \in \mathbb{G}M^n (g_k \times [0, h], G)} \\ & \Phi^{-1} \left(L_{g_k^{-1}} g_n(0) \right) = \xi_k, \Phi^{-1} \left(L_{g_k^{-1}} g_n(h) \right) = \xi_{k+1} \\ & h \sum_{j=1}^m b_j L (g_n (c_j h), \dot{g}_n (c_j h)) \end{aligned}$$

and compare it to the discrete Lagrangian on the Lie group,

$$L_d (g_k, g_{k+1}, h) = \text{ext}_{\substack{g_n \in \mathbb{G}M^n (g_k \times [0, h], G) \\ g_n(0) = g_k, g_n(h) = g_{k+1}}} h \sum_{j=1}^m b_j L (g_n (c_j h), \dot{g}_n (c_j h))$$

it can be seen that there is a simple one-to-one correspondence through the natural charts between points in $G \times G$ and points in $\mathfrak{g} \times \mathfrak{g}$, and that if $(\Phi^{-1} (L_{g_k^{-1}} g_0), \Phi^{-1} (L_{g_k^{-1}} g_1)) = (\xi_0, \xi_1)$, then

$$L (g_0, g_1) = \hat{L}_d (\xi_0, \xi_1).$$

Hence, for every sequence $\{g_k\}_{k=1}^N$, there exists a unique sequence $\{\xi_k\}_{i=1}^N$ such that

$$\sum_{k=1}^{N-1} L_d (g_k, g_{k+1}) = \sum_{k=1}^{N-1} \hat{L}_d (\xi_k, \xi_{k+1}), \tag{5}$$

and vice versa. Thus, we can find the sequence $\{g_k\}_{k=1}^N$ that makes the sum on the left-hand side of (5) stationary by finding the sequence $\{\xi_k\}_{k=1}^N$ that makes the sum on the right-hand side of (5) stationary.

It can easily be seen that the stationarity condition of the action sum on the right is

$$D_2 \hat{L}_d (\xi_{k-1}, \xi_k) + D_1 \hat{L}_d (\xi_k, \xi_{k+1}) = 0. \tag{6}$$

However, from the definition of \hat{L}_d , this implicitly assumes that (ξ_{k-1}, ξ_k) and (ξ_k, ξ_{k+1}) are in the same natural chart. Unfortunately, in our construction (ξ_{k-1}, ξ_k) and (ξ_k, ξ_{k+1}) are in different natural charts. This is because the construction of the Lie group interpolating curve

$$g(t) = L_{g_\beta} \Phi \left(\sum_{i=1}^n \xi_k^i \phi_i(t) \right)$$

requires the choice of a base point for the natural chart $g_\beta \in G$. If a consistent choice of base point was made for each time-step, then the above equations could be directly computed without difficulty. However, because many natural chart functions contain coordinate singularities, our construction uses a different base point, and thus a different natural chart, at each time-step. Specifically, on the interval $[kh, (k + 1)h]$, we choose $g_\beta = g_k$ and define

$$g(t) = L_{g_k} \Phi \left(\sum_{i=1}^n \xi_k^i \phi_i(t) \right).$$

Thus

$$g(t) = L_{g_{k-1}} \Phi \left(\sum_{j=1}^n \xi_{k-1}^j \phi_j(t) \right), t \in [(k - 1)h, kh]$$

$$g(t) = L_{g_k} \Phi \left(\sum_{j=1}^n \xi_k^j \phi_j(t) \right), t \in [kh, (k + 1)h],$$

where we now denote internal stage points ξ_k^i with the subscript k to denote in which interval they occur. While the change in natural chart is expedient for the construction, it creates a difficulty for the computation of the discrete Euler–Lagrange equations, in that now we are using discrete Lagrangians with different natural charts for the different time-steps, and hence we cannot compute the discrete Euler–Lagrange equations using (6). This problem can be resolved by expressing $g(t)$, and hence (ξ_{k-1}, ξ_k) and (ξ_k, ξ_{k+1}) , in the same natural chart for $t \in [(k - 1)h, (k + 1)h]$. Rewriting

$$g_n(t) = L_{g_k} \Phi \left(\sum_{i=1}^n \xi_k^i \phi_i(t) \right)$$

$$= L_{g_{k-1}} \Phi \left(\Phi^{-1} \left(L_{g_{k-1}}^{-1} L_{g_k} \Phi \left(\sum_{i=1}^n \xi_k^i \phi_i(t) \right) \right) \right), t \in [kh, (k + 1)h],$$

(note that $g_n(t)$ is still in $\mathbb{GM}^n(g_k \times [0, h], G)$), and defining

$$\lambda(t) = \Phi^{-1} \left(L_{g_{k-1}} L_{g_k} \Phi \left(\sum_{i=1}^n \xi_k^i \phi_i(t) \right) \right) = \Phi^{-1} \left(L_{\Phi(\xi_k)} \Phi \left(\sum_{i=1}^n \xi_k^i \phi_i(t) \right) \right)$$

we can reexpress the discrete Lagrangian as

$$\begin{aligned} \tilde{L}_d(\lambda_k, \lambda_{k+1}) = & \text{ext}_{g_n \in \mathbb{GM}^n(g_k \times [0, h], G)} \\ & \Phi^{-1} \left(L_{g_{k-1}} g_n(0) \right) = \lambda_k, \Phi^{-1} \left(L_{g_{k-1}} g_n(h) \right) = \lambda_{k+1} \\ & h \sum_{j=1}^m b_j L(g_n(c_j h), \dot{g}_n(c_j h)). \end{aligned}$$

Note that if $L_{g_{k-1}} \Phi(\lambda_k) = L_{g_k} \Phi(\xi_k)$ and $L_{g_{k-1}} \Phi(\lambda_{k+1}) = L_{g_k} \Phi(\xi_{k+1})$ that

$$\hat{L}_d(\xi_k, \xi_{k+1}) = \tilde{L}_d(\lambda_k, \lambda_{k+1}).$$

Furthermore, $(\lambda_k, \lambda_{k+1})$ are in the same chart as (ξ_{k-1}, ξ_k) , and hence the discrete Euler–Lagrange equations are

$$D_2 \hat{L}_d(\xi_{k-1}, \xi_k) + D_1 \tilde{L}_d(\lambda_k, \lambda_{k+1}) = 0.$$

It remains to compute λ_k as a function of ξ_k . If we consider the definition of $\lambda(t)$, then

$$\lambda_k = \lambda(0) = \Phi^{-1} \left(L_{\Phi(\xi_k)} \Phi \left(\sum_{i=1}^n \xi_k^i \phi_i(0) \right) \right)$$

and

$$\xi_k = \Phi^{-1} \left(L_{g_k^{-1}} g_n(0) \right) = \Phi^{-1} \left(L_{\Phi(\xi_k)^{-1}} \Phi(\lambda_k) \right). \tag{7}$$

This is simply a change of coordinates, and hence computing the discrete Euler Lagrange equations amounts to using the change of coordinates map to transform the algebra elements into the same chart. Thus,

$$\begin{aligned} D_2 \hat{L}_d(\xi_{k-1}, \xi_k) &= \frac{\partial L_d}{\partial \xi_k} \\ D_1 \tilde{L}_d(\lambda_k, \lambda_{k+1}) &= \frac{\partial L_d}{\partial \xi_k} \frac{\partial \xi_k}{\partial \lambda_k} \end{aligned} \tag{8}$$

where (7) can be used to compute $\frac{\partial \xi_k}{\partial \lambda_k}$. An explicit example is presented in section Sect. 4.

There are several features of this computation that should be noted. First, since we are considering specific choices of natural charts, we may think of ξ_k and λ_k as corresponding to a specific coordinate choice, and hence it is natural to use standard partial derivatives as opposed to coordinate-free notation. Second, because λ_k is a function of ξ_k , which is in turn a function of ξ_k^i , this is still a root-finding problem over ξ_k^i and hence may be solved concurrently with the internal stage Euler–Lagrange equations (3).

3 Convergence

Thus far, we have discussed the construction of Lie group Galerkin variational integrators—now we will prove several theorems related to their convergence. Unlike traditional numerical methods for differential equations, we will achieve convergence in two distinct ways.

- (1) *h-refinement* Shortening of the time-step h while holding the dimension of the function space $\mathbb{GM}^n(g_0 \times [0, h], G)$ constant, which we refer to as *h-refinement*. In practice, we refer to methods that achieve convergence through *h-refinement* as *Lie group Galerkin variational integrators*, after the framework used to construct them.
- (2) *n-refinement* Increasing the dimension of the function space $\mathbb{GM}^n(g_0 \times [0, h], G)$ while holding the time-step h constant. Because enriching $\mathbb{GM}^n(g_0 \times [0, h], G)$ involves increasing the number of basis functions, and hence the value of n , we refer to this as *n-refinement*. Because this approach of enriching the function space is inspired by classical spectral methods, as in Trefethen [38], when we use *n-refinement* to achieve convergence we will refer to the resulting method as a *Lie group spectral variational integrator*.

3.1 Geometric and High-Order Convergence

Naturally, the goal of applying the spectral paradigm to the construction of Galerkin variational integrators is to construct methods which achieve geometric convergence. In this section, we will prove that under certain assumptions about the behavior of the Lagrangian and the approximation space, Lie group spectral variational integrators achieve geometric convergence. Additionally, the argument that establishes geometric convergence can be easily modified to show that arbitrarily high-order Lie group Galerkin integrators can be constructed.

The proof of the rate of convergence Galerkin Lie group variational integrators is superficially similar to the proof of the rate of convergence of Galerkin variational integrators, which was established in [13]. The specific major difference is the need to quantify the error between two different curves on the Lie group. Unlike a normed vector space, where the error can be quantified by taking the difference between the exact solution and the approximate solution, there may not be a simple method of quantifying the error of an approximate solution that evolves in a Lie group. For the moment, we will avoid this difficulty by assuming that the error between two curves

that share a common point in a Lie group can be bounded by the error between curves in the Lie algebra. Since Lie algebras are vector spaces, the error between a curve through the Lie algebra and an approximation to that curve can be measured by taking the difference between the two curves and using a norm induced by an appropriate metric.

With this requirement in mind, we define the “natural chart conditioning” assumption. Given placeholder functions (for practical applications, these functions should be chosen appropriately for the specific problem):

- (1) $e_g(\cdot, \cdot)$, which measures the error between two curves through the Lie group,
- (2) $e_a(\cdot, \cdot)$, which measures the error between two curves through the tangent bundle of the Lie group,

we define the *natural chart conditioning assumption* as follows

$$e_g(L_{g_0}\Phi(\xi(t)), L_{g_0}\Phi(\eta(t))) \leq C_G \langle \xi(t) - \eta(t), \xi(t) - \eta(t) \rangle^{\frac{1}{2}} \tag{9}$$

$$e_a\left(\frac{d}{dt}L_{g_0}\Phi(\xi(t)), \frac{d}{dt}L_{g_0}\Phi(\eta(t))\right) \leq C_g \langle \dot{\xi}(t) - \dot{\eta}(t), \dot{\xi}(t) - \dot{\eta}(t) \rangle^{\frac{1}{2}} + C_g^G \langle \xi(t) - \eta(t), \xi(t) - \eta(t) \rangle^{\frac{1}{2}} \tag{10}$$

where $\langle \cdot, \cdot \rangle$ is a Riemannian metric on the Lie algebra. This essentially states that the error between two curves in the Lie group is bounded by the error of those curves when reduced to curves in the Lie algebra.

While the length of the geodesic curve that connects $L_{g_k}\Phi(\xi)$ and $L_{g_k}\Phi(\eta)$ is an obvious choice for the error function $e_g(\cdot, \cdot)$, it is important to note that there are other valid choices. This will greatly simplify error calculations; for example, in Sect. 4 we choose the error function to be the matrix two-norm, $\|\cdot\|_2$, which is quickly and easily computed and will obey this inequality for the Riemannian metric we use.

3.1.1 Arbitrarily High-Order Convergence

We will begin by proving that Lie group Galerkin variational integrators can be constructed that are of arbitrarily high order. The proof that follows is involved and may be daunting at first glance, so we provide a general qualitative outline of it here to guide the interested reader.

We begin by making several key assumptions about the properties of the Lagrangian, approximation space, and choice of error functions. Specifically, we assume

- (1) *Sufficiently short evolution* the exact solution over the given time interval is contained within the range of the natural chart function,
- (2) *High-quality approximation space* there exists a high-order approximation to the true solution in the approximation space (we may not be able to compute it explicitly—it just must exist theoretically),
- (3) *Regular Lagrangian* the Lagrangian is sufficiently smooth,
- (4) *Well-conditioned natural chart* the natural chart is well conditioned, as discussed in (9) and (10),

- (5) *Quadrature accuracy* the quadrature rule we choose to construct the integrator is sufficiently accurate,
- (6) *Minimizing stationary points* the stationary points of both the discrete action (used to construct the variational integrator) and the exact action (used to define the equations of motion), are minimizers.

Using these assumptions, we establish convergence by computing the error between the discrete Galerkin discrete Lagrangian used to construct our methods and the exact discrete Lagrangian. We do this by

- (1) *Bounding the difference between the exact action evaluated on the theoretical high-order approximation and the exact solution* Using our assumption about the regularity of the Lagrangian to bound the difference between the value of the exact action evaluated on the exact solution and the value of the exact action evaluated on the theoretical high-order solution in the approximation space,
- (2) *Bounding the difference between the approximate action on the theoretical high-order approximation and the computable Galerkin approximation* Using our assumption that the stationary point of the approximate action is a minimizer to bound the difference between the value of the approximate action on the Galerkin approximation and the value of the approximate action on the theoretical high-order approximation,
- (3) *Bounding the difference between the approximate action and exact action on the theoretical high-order approximation* Using our assumption on the accuracy of the quadrature rule to bound the difference between the exact action and the approximate action on the theoretical high-order approximation,
- (4) *Combining the bounds* Using the three bounds to bound the difference between the Galerkin discrete Lagrangian and the exact discrete Lagrangian.

Since Theorem 1.1 establishes a bound on the error of the one-step map from the error of the discrete Lagrangian, the error between the discrete Galerkin Lagrangian and the exact discrete Lagrangian can be used to establish error bounds for the resulting numerical method.

The careful reader will note that we have made a slight abuse of notation; in Sect. 2, we used n to denote the number of basis points used to construct our interpolation functions, while in the proofs that follow, we use n as a parameter to bound the error of approximations in the chosen approximation space. While these two values are not necessarily the same, in practice the bound on the error of the approximations in the approximation space is related to the number of basis points used to construct the approximation space. We will be careful to point out where they are different in our numerical examples.

Theorem 3.1 *Given an interval $[0, h]$, and a Lagrangian $L : TG \rightarrow \mathbb{R}$, suppose that $\bar{g}(t)$ solves the Euler–Lagrange equations on that interval exactly. Furthermore, suppose that the exact solution $\bar{g}(t)$ falls within the range of the natural chart (**sufficiently short evolution**), that is:*

$$\bar{g}(t) = L_{g_k} \Phi(\bar{\eta}(t))$$

for some $\bar{\eta}(t) \in C^2([0, h], \mathfrak{g})$. For the function space $\mathbb{GM}^n(g_0 \times [0, h], G)$ and the quadrature rule \mathcal{G} , define the Galerkin discrete Lagrangian $L_d^G(g_0, g_1) \rightarrow \mathbb{R}$ as

$$\begin{aligned}
 L_d^G(g_0, g_1, h) &= \underset{\substack{g_n \in \mathbb{GM}^n(g_0 \times [0, h], G) \\ g_n(0) = g_0, g_n(h) = g_1}}{\text{ext}} h \sum_{j=1}^m b_j L(g_n(c_j h), \dot{g}_n(c_j h)) \\
 &= h \sum_{j=1}^m b_j L(\tilde{g}_n(c_j h), \dot{\tilde{g}}_n(c_j h))
 \end{aligned} \tag{11}$$

where $\tilde{g}_n(t)$ is the extremizing curve in $\mathbb{GM}^n(g_0 \times [0, h], G)$. If:

- (1) (**High-quality approximation space**) there exists an approximation $\hat{\eta}_n \in \mathbb{M}^n([0, h], \mathfrak{g})$ such that,

$$\begin{aligned}
 \left\langle \bar{\eta}(t) - \hat{\eta}_n(t), \bar{\eta}(t) - \hat{\eta}_n(t) \right\rangle^{\frac{1}{2}} &\leq C_A h^n \\
 \left\langle \dot{\bar{\eta}}(t) - \dot{\hat{\eta}}_n(t), \dot{\bar{\eta}}(t) - \dot{\hat{\eta}}_n(t) \right\rangle^{\frac{1}{2}} &\leq C_{\mathfrak{A}} h^n,
 \end{aligned}$$

for some constants $C_A \geq 0$ and $C_{\mathfrak{A}} \geq 0$ independent of h ,

- (2) (**Regular Lagrangian**) the Lagrangian L is Lipschitz in the chosen norms in both its arguments, that is:

$$|L(g_1, \dot{g}_1) - L(g_2, \dot{g}_2)| \leq L_\alpha (e_g(g_1, g_2) + e_a(\dot{g}_1, \dot{g}_2)),$$

- (3) (**Well-conditioned natural chart**) the chart function Φ is well conditioned in $e_g(\cdot, \cdot)$ and $e_a(\cdot, \cdot)$, that is (9) and (10) hold,
- (4) (**Quadrature accuracy**) for the quadrature rule $\mathcal{G}(f) = h \sum_{j=1}^m b_j f(c_j h) \approx \int_0^h f(t) dt$, there exists a constant $C_g \geq 0$ such that,

$$\left| \int_0^h L(g_n(t), \dot{g}_n(t)) dt - h \sum_{j=1}^m b_j L(g_n(c_j h), \dot{g}_n(c_j h)) \right| \leq C_g h^{n+1}$$

for any $g_n(t) = L_{g_0} \Phi(\xi(t))$ where $\xi \in \mathbb{M}^n([0, h], \mathfrak{g})$,

- (5) (**Minimizing stationary points**) the stationary points of the discrete action and the continuous action are minimizers,

then the variational integrator induced by $L_d^G(g_0, g_1)$ has error $\mathcal{O}(h^{n+1})$.

Proof We begin by rewriting the exact discrete Lagrangian and the Galerkin discrete Lagrangian:

$$\begin{aligned} & \left| L_d^E(g_0, g_1, h) - L_d^G(g_0, g_1, h) \right| \\ &= \left| \int_0^h L(\bar{g}, \dot{\bar{g}}) dt - h \sum_{j=1}^m b_j L(\bar{g}_n(c_j h), \dot{\bar{g}}_n(c_j h)) \right|, \end{aligned}$$

where we have introduced $\tilde{g}_n(t)$, which is the stationary point of the local Galerkin action (11). We begin by bounding the difference between the action evaluated on the exact solution, which is another expression of the exact discrete Lagrangian, and the action evaluated on the theoretical high-order approximation to the exact solution, step 1 of our qualitative outline. We introduce the theoretical high-order solution in the approximation space, which takes the form $\hat{g}_n(t) = L_{g_k} \Phi(\hat{\eta}_n(t))$, and compare the action evaluated on the exact solution to the action evaluated on this solution:

$$\begin{aligned} \left| \int_0^h L(\bar{g}, \dot{\bar{g}}) dt - \int_0^h L(\hat{g}_n, \dot{\hat{g}}_n) dt \right| &= \left| \int_0^h L(\bar{g}, \dot{\bar{g}}) - L(\hat{g}_n, \dot{\hat{g}}_n) dt \right| \\ &\leq \int_0^h \left| L(\bar{g}, \dot{\bar{g}}) - L(\hat{g}_n, \dot{\hat{g}}_n) \right| dt. \end{aligned}$$

Now, we use the Lipschitz assumption (assumption 2) to establish the bound

$$\begin{aligned} & \int_0^h \left| L(\bar{g}, \dot{\bar{g}}) - L(\hat{g}_n, \dot{\hat{g}}_n) \right| dt \\ & \leq \int_0^h L_\alpha \left(e_g(\bar{g}, \hat{g}_n) + e_a(\dot{\bar{g}}, \dot{\hat{g}}_n) \right) dt \\ & = \int_0^h L_\alpha \left(e_g(L_{g_k} \Phi(\bar{\eta}), L_{g_k} \Phi(\hat{\eta}_n)) \right. \\ & \quad \left. + e_a(D_{\Phi(\bar{\eta})} L_{g_0} D_{\bar{\eta}} \Phi(\dot{\bar{\eta}}), D_{\Phi(\hat{\eta}_n)} L_{g_0} D_{\hat{\eta}_n} \Phi(\dot{\hat{\eta}}_n)) \right) dt. \end{aligned}$$

Next, we use the chart conditioning assumptions (assumption 3) to establish the bound

$$\begin{aligned} \int_0^h \left| L(\bar{g}, \dot{\bar{g}}) - L(\hat{g}_n, \dot{\hat{g}}_n) \right| dt &\leq \int_0^h L_\alpha \left(C_G \langle \bar{\eta} - \hat{\eta}_n, \bar{\eta} - \hat{\eta}_n \rangle^{\frac{1}{2}} + C_g \langle \dot{\bar{\eta}} - \dot{\hat{\eta}}_n, \dot{\bar{\eta}} - \dot{\hat{\eta}}_n \rangle^{\frac{1}{2}} \right. \\ & \quad \left. + C_g^G \langle \bar{\eta} - \hat{\eta}, \bar{\eta} - \hat{\eta} \rangle^{\frac{1}{2}} \right) dt \\ &\leq \int_0^h L_\alpha \left(C_G C_A h^n + C_g C_{\mathfrak{A}} h^n + C_g^G C_A h^n \right) dt \\ &= L_\alpha \left((C_G + C_g^G) C_A + C_g C_{\mathfrak{A}} \right) h^{n+1}. \end{aligned}$$

This establishes a bound between the exact action evaluated on the true solution (which yields the exact discrete Lagrangian) and the theoretical high-order approximation in the approximation space, \hat{g}_n . Next, we move on to step 2, step 3, and step 4 of our proof, establishing a bound between the approximate action evaluated on our computable

Galerkin approximation and the high-order approximation, computing a bound on the difference between the approximate action and the exact action evaluated on the theoretical high-order approximation, and then using these bounds to compute a bound on the error of the discrete Lagrangian. Considering the Galerkin discrete action,

$$\begin{aligned}
 h \sum_{j=1}^m b_j L(\tilde{g}_n, \dot{\tilde{g}}_n) &\leq h \sum_{j=1}^m b_j L(\hat{g}_n, \dot{\hat{g}}_n) \\
 &\leq \int_0^h L(\hat{g}_n, \dot{\hat{g}}_n) dt + C_g h^{n+1} \\
 &\leq \int_0^h L(\bar{g}, \dot{\bar{g}}) dt + C_g h^{n+1} + L_\alpha \left((C_G + C_g^G) C_A + C_g C_{\mathfrak{A}} \right) h^{n+1}
 \end{aligned}
 \tag{12}$$

where we have used the assumption that the Galerkin approximation \tilde{g}_n minimizes the Galerkin discrete action (assumption 5) and the assumption on the accuracy of the quadrature (assumption 4). Now, using the fact that $\bar{g}(t)$ minimizes the action and that $\mathbb{GM}^n(g_0 \times [0, h], G) \subset C^2([0, h], G)$ (assumption 5 again),

$$\begin{aligned}
 h \sum_{j=1}^m b_j L(\tilde{g}_n, \dot{\tilde{g}}_n) &\geq \int_0^h L(\tilde{g}_n, \dot{\tilde{g}}_n) dt - C_g h^{n+1} \\
 &\geq \int_0^h L(\bar{g}, \dot{\bar{g}}) dt - C_g h^{n+1}
 \end{aligned}
 \tag{13}$$

Combining inequalities (12) and (13), we see that,

$$\begin{aligned}
 \int_0^h L(\bar{g}, \dot{\bar{g}}) dt - C_g h^{n+1} &\leq h \sum_{j=1}^m b_j L(\tilde{g}_n, \dot{\tilde{g}}_n) \\
 &\leq \int_0^h L(\bar{g}, \dot{\bar{g}}) dt + C_g h^{n+1} + L_\alpha \left((C_G + C_g^G) C_A + C_g C_{\mathfrak{A}} \right) h^{n+1}
 \end{aligned}$$

which implies

$$\left| \int_0^h L(\bar{g}, \dot{\bar{g}}) dt - h \sum_{j=1}^m b_j L(\tilde{g}_n, \dot{\tilde{g}}_n) \right| \leq \left(C_g + L_\alpha \left((C_G + C_g^G) C_A + C_g C_{\mathfrak{A}} \right) \right) h^{n+1}.
 \tag{14}$$

The left-hand side of (14) is exactly $|L_d^E(g_0, g_1, h) - L_d^G(g_0, g_1, h)|$, and thus

$$\left| L_d^E(g_0, g_1, h) - L_d^G(g_0, g_1, h) \right| \leq C_{op} h^{n+1}$$

where

$$C_{op} = C_g + L_\alpha \left((C_G + C_g^G) C_A + C_g C_{\mathfrak{A}} \right).$$

This states that the Galerkin discrete Lagrangian approximates the exact discrete Lagrangian with error $\mathcal{O}(h^{n+1})$, and by Theorem (1.1) this further implies that the Lagrangian update map, and hence the Lie group Galerkin variational integrator has error $\mathcal{O}(h^{n+1})$. □

3.1.2 Geometric Convergence

Under similar assumptions, we can demonstrate that Lie group spectral variational integrators will converge geometrically with n -refinement, that is, enrichment of the function space $\mathbb{GM}^n(g_0 \times [0, h], G)$ as opposed to the shortening of the time-step h . The fundamental assumptions and technique of the proof is essentially the same as the proof of arbitrarily high-order convergence: assuming that the Lagrangian is sufficiently regular, that the approximation space and the quadrature rule are sufficiently accurate, that the natural chart is well conditioned and that the exact solution of the system does not exceed the range of the natural chart, the curve that results from solving the discrete Euler–Lagrange equations will converge geometrically as the dimension of the approximation space is increased. A notable difference between the statement of the previous theorem and this one is that the order of the quadrature rule must be increased along with the dimension of the approximation space in order to achieve convergence—this is because once the approximation space becomes sufficiently accurate, it is the order of the quadrature rule that introduces the most significant source of error, and only by increasing the order of the quadrature rule can one achieve the desired rate of convergence.

Theorem 3.2 *Given an interval $[0, h]$, and a Lagrangian $L : TG \rightarrow \mathbb{R}$, suppose that $\bar{g}(t)$ solves the Euler–Lagrange equations on that interval exactly. Furthermore, suppose that the exact solution $\bar{g}(t)$ falls within the range of the natural chart (**sufficiently short evolution**), that is:*

$$\bar{g}(t) = L_{g_k} \Phi(\bar{\eta}(t))$$

for some $\bar{\eta} \in C^2([0, h], \mathfrak{g})$. For the function space $\mathbb{M}^n([0, h], \mathfrak{g})$ and the quadrature rule \mathcal{G} , define the Galerkin discrete Lagrangian $L_d^G(g_0, g_1) \rightarrow \mathbb{R}$ as

$$\begin{aligned} L_d^G(g_0, g_1, h) &= \underset{\substack{g_n \in \mathbb{GM}^n(g_0 \times [0, h], G) \\ g_n(0) = g_0, g_n(h) = g_1}}{\text{ext}} h \sum_{j=1}^m b_j L(g_n(c_j h), \dot{g}_n(c_j h)) \\ &= h \sum_{h=1}^m b_j L(\tilde{g}_n(c_j h), \dot{\tilde{g}}_n(c_j h)) \end{aligned} \tag{15}$$

where $\tilde{g}_n(t)$ is the extremizing curve in $\mathbb{GM}^n(g_0 \times [0, h], G)$. If:

- (1) (**High-quality approximation space**) there exists an approximation $\hat{\eta}_n \in \mathbb{M}^n([0, h], \mathfrak{g})$ such that,

$$\begin{aligned} \langle \bar{\eta} - \hat{\eta}_n, \bar{\eta} - \hat{\eta}_n \rangle^{\frac{1}{2}} &\leq C_A K_A^n \\ \langle \dot{\bar{\eta}} - \dot{\hat{\eta}}_n, \dot{\bar{\eta}} - \dot{\hat{\eta}}_n \rangle^{\frac{1}{2}} &\leq C_{\mathfrak{A}} K_A^n, \end{aligned}$$

for some constants $C_A \geq 0$ and $C_{\mathfrak{A}} \geq 0$, $0 < K_A < 1$ independent of n ,

- (2) (**Regular Lagrangian**) the Lagrangian L is Lipschitz in the chosen error norm in both its arguments, that is:

$$|L(g_1, \dot{g}_1) - L(g_2, \dot{g}_2)| \leq L_\alpha (e_g(g_1, g_2) + e_a(\dot{g}_1, \dot{g}_2))$$

- (3) (**Well-conditioned natural chart**) the chart function Φ is well conditioned in $e_g(\cdot, \cdot)$ and $e_a(\cdot, \cdot)$, that is (9) and (10) hold,
 (4) (**Quadrature accuracy**) there exists a sequence of quadrature rules $\{\mathcal{G}_n\}_{n=1}^\infty$, $\mathcal{G}_n(f) = h \sum_{j=1}^{m_n} b_{nj} f(c_{nj}h) \approx \int_0^h f(t) dt$, and there exists a constant $0 < K_g < 1$ independent of n such that,

$$\left| \int_0^h L(g_n(t), \dot{g}_n(t)) dt - h \sum_{j=1}^m b_j L(g_n(c_jh), \dot{g}_n(c_jh)) \right| \leq C_g K_g^n$$

for any $g_n(t) = L_{g_0} \Phi(\xi(t))$ where $\xi \in \mathbb{M}^n([0, h], \mathfrak{g})$,

- (5) (**Minimizing stationary points**) the stationary points of the discrete action and the continuous action are minimizers,

then the variational integrator induced by $L_d^G(g_0, g_1)$ has error $\mathcal{O}(K^n)$.

The proof for this theorem is very similar to that for Theorem 3.1, using the modified assumptions in the obvious way. It would be tedious to repeat it here, but it has been included in the ‘‘Appendix’’ for completeness.

These proofs may seem quite strong in their assumptions. However, many of the assumptions can be viewed as design guidelines for constructing an integrator: In order to achieve high-order or geometric convergence with a Lie group Galerkin variational integrator, one must be careful when selecting the approximation space, quadrature rule, and natural chart used in its construction. As we shall see in Sect. 4, there are many reasonable choices of function spaces, natural chart functions, quadrature rules and error norms such that the assumptions are satisfied. The more difficult assumption is the minimizers assumption, that the stationary points of both the discrete and exact actions are minimizers. While this may not hold in general, we will show here that for a large class of Lagrangians of interest, this assumption holds. We will specifically examine Lagrangians over $SO(3)$ of the form:

$$L(R, \dot{R}) = \text{tr}(\dot{R}^T R J_d R^T \dot{R}) - V(R), \tag{16}$$

where $R \in SO(3)$, which is the rigid body under the influence of a potential. We will show that for Lie group Galerkin variational integrators, stationary points of the discrete action are minimizers under a certain time-step restriction. In addition, in Sect. 4 we will give a specific construction of a Lie group Galerkin variational integrator for this type of problem, and demonstrate the expected convergence on several example problems.

3.2 Stationary Points are Minimizers

A major assumption in both Theorem 3.1 and Theorem 3.2 is that the stationary point of the discrete action is a minimizer. While in general this may not hold, we can show that given a time-step restriction on h , that this condition holds for problems on $SO(3)$ for Lagrangians of the form

$$L(R, \dot{R}) = \text{tr}(\dot{R}^T R J_d R^T \dot{R}) - V(R).$$

This includes a broad range of problems. Furthermore, we establish a similar result for problems in vector space in Hall and Leok [13], and it may be possible to combine these two results to include a large class of problems, including those that evolve on the special Euclidean group $SE(3) = \mathbb{R}^3 \times SO(3)$.

Again, the proof of the following lemma may seem daunting at first glance. This is due to the fact that the Lagrangian maps curves in the tangent bundle of the Lie group to the real numbers, and hence in order to exploit the vector space structure of the Lie algebra, we must apply a mapping from the Lie algebra into the Lie group. This mapping adds necessary complication; however, behind this complication is a relatively straightforward idea: When the time-step is sufficiently short, the action of the Lagrangian (16) can be approximated by the difference of between the integral of a quadratic form on a curve through \mathbb{R}^3 and the integral of a quadratic form on its derivative. Since both quadratic forms are positive-definite, we can make use of the Poincaré inequality to show that the integral of the quadratic form on the derivative dominates the integral quadratic form on the curve itself, and this results in their difference being strictly increasing around the stationary point, which implies the stationary point is a minimizer.

Furthermore, since we are examining the stationary points on functionals that map sufficiently smooth curves to the reals, we must appeal to functional analysis to provide the machinery to complete the proof. This means that where finite-dimensional analysis might use the standard gradient or Hessian, we make use of the first and second Frechet derivative in order to extend the arguments about minimization. However, the overall idea remains the same—in a broad sense, we are simply demonstrating that the integral of one quadratic form dominates another.

Lemma 3.1 *Consider a Lagrangian on $SO(3)$ of the form*

$$L(R, \dot{R}) = \text{tr}(\dot{R}^T R J_d R^T \dot{R}) - V(R),$$

where $R \in SO(3)$ and J_d is a diagonal matrix with $j_{ii} > 0$ for all i , and V is a smooth function on $SO(3)$. If a Lie group Galerkin variational integrator is constructed with $\{\phi_i\}_{i=1}^n$ forming the basis for polynomials of degree $n + 1$ and the quadrature rule is of order at least $2n + 2$, then the stationary points of the discrete action are minimizers.

Proof We begin by noting that we can identify every element of $\mathfrak{so}(3)$, the Lie algebra associated with $SO(3)$, with an element of \mathbb{R}^3 using the hat map $\hat{\cdot} : \mathbb{R}^3 \rightarrow \mathfrak{so}(3)$,

$$\widehat{\begin{pmatrix} a \\ b \\ c \end{pmatrix}} = \begin{pmatrix} 0 & -c & b \\ c & 0 & -a \\ -b & a & 0 \end{pmatrix}. \tag{17}$$

Hence, it is natural to consider the discrete action as a function on $H^1([0, h], \mathbb{R}^3)$,

$$\mathbb{S}_d(\xi(t), \dot{\xi}(t)) = h \sum_{j=1}^m b_j L \left(L_{g_k} \Phi(\hat{\xi}(c_j h)), \frac{d}{dt} L_{g_k} \Phi(\hat{\xi}(c_j h)) \right),$$

where $\xi(t) \in H^1([0, h], \mathbb{R}^3)$. Let $\check{\xi}(t)$ be the stationary point of \mathbb{S}_d in the space

$$\left\{ \xi(t) \mid \xi(t) \in H^1([0, h], \mathbb{R}^3), \xi(0) = \xi_0, \xi(h) = \xi_h \right\},$$

which is exactly the type of space we seek to extremize the action over when constructing our discrete Lagrangian. Now, consider a perturbation to $\check{\xi}(t)$ in this space, $\check{\xi}(t) + \delta\xi(t)$. Since $\check{\xi}(t)$ is the extremizer over curves $\xi(t)$ subject to the constraints $\xi(0) = \xi_0, \xi(h) = \xi_h$, we know $\delta\xi(0) = 0$ and $\delta\xi(h) = 0$, but it is otherwise arbitrary. Hence, we consider an arbitrary perturbation $\delta\xi(t) \in H_0^1([0, h], \mathbb{R}^3)$. Since \mathbb{S}_d is a function on $H^1([0, h], \mathbb{R}^3)$, we can Taylor expand around the stationary point:

$$\begin{aligned} \mathbb{S}_d(\check{\xi} + \delta\xi, \dot{\check{\xi}} + \delta\dot{\xi}) &= \mathbb{S}_d(\check{\xi}, \dot{\check{\xi}}) + D\mathbb{S}_d(\check{\xi}, \dot{\check{\xi}})[(\delta\xi, \delta\dot{\xi})] \\ &\quad + \frac{1}{2} D^2\mathbb{S}_d(\eta, \dot{\eta})[(\delta\xi, \delta\dot{\xi})][(\delta\xi, \delta\dot{\xi})] \end{aligned}$$

where $\eta(t) = \lambda(t)\xi_0(t) + (1 - \lambda(t))\delta\xi(t)$ for some $\lambda(t) : [0, h] \rightarrow [0, 1]$ and $D\mathbb{S}_d, D^2\mathbb{S}_d$ are the first and second Frechet derivative of \mathbb{S}_d , respectively. One can think of the curve $\eta(t)$ as being the infinite-dimensional analogue to the intermediate point in the remainder of the familiar finite-dimensional Taylor theorem. Thus

$$\begin{aligned} \mathbb{S}_d(\check{\xi} + \delta\xi, \dot{\check{\xi}} + \delta\dot{\xi}) - \mathbb{S}_d(\check{\xi}, \dot{\check{\xi}}) &= D\mathbb{S}_d(\check{\xi}, \dot{\check{\xi}})[(\delta\xi, \delta\dot{\xi})] \\ &\quad + \frac{1}{2} D^2\mathbb{S}_d(\eta, \dot{\eta})[(\delta\xi, \delta\dot{\xi})][(\delta\xi, \delta\dot{\xi})]. \end{aligned}$$

Now, note that

$$D\mathbb{S}_d(\check{\xi}, \dot{\check{\xi}})[(\delta\xi, \delta\dot{\xi})] = 0$$

for arbitrary $\delta\xi(t)$ is exactly the stationarity conditions for the internal stage discrete Euler–Lagrange equations, and thus the first Frechet derivative vanishes at the stationary point. Therefore,

$$\mathbb{S}_d(\check{\xi} + \delta\xi, \check{\xi} + \delta\dot{\xi}) - \mathbb{S}_d(\check{\xi}, \check{\xi}) = \frac{1}{2} D^2\mathbb{S}_d(\eta, \dot{\eta}) [(\delta\xi, \delta\dot{\xi})] [(\delta\xi, \delta\dot{\xi})].$$

We will examine $D^2\mathbb{S}_d$. The second Frechet derivative of the discrete action is given by

$$D^2\mathbb{S}_d(\xi, \dot{\xi}) [(\delta\xi_a, \delta\dot{\xi}_a)] [(\delta\xi_b, \delta\dot{\xi}_b)] = h \sum_{j=1}^m b_j \nabla^2 L(\xi, \dot{\xi}) [(\delta\xi_a(c_jh), \delta\dot{\xi}_a(c_jh))] [(\delta\xi_b(c_jh), \delta\dot{\xi}_b(c_jh))].$$

In order to examine the second Frechet derivative, we must examine the Hessian of the Lagrangian. We will do this term wise. The Lagrangian has the form

$$L(\xi, \dot{\xi}) = K(\xi, \dot{\xi}) - V(\xi)$$

where

$$K(\xi(t), \dot{\xi}(t)) = \dot{R}(\xi(t))^T R(\xi(t)) J_d R(\xi(t))^T \dot{R}(\xi(t))$$

is the kinetic energy and V is the potential energy, and from this it follows that

$$\nabla^2 L(\xi, \dot{\xi}) [\cdot, \cdot] = \nabla^2 K(\xi, \dot{\xi}) [\cdot, \cdot] - \nabla^2 V(\xi, \dot{\xi}) [\cdot, \cdot].$$

With careful analysis, the following bound can be established on $\nabla^2 K$,

$$\nabla^2 K(\eta(t), \dot{\eta}(t)) [(\delta\xi, \delta\dot{\xi})] [(\delta\xi, \delta\dot{\xi})] \geq C_{\xi} \delta\dot{\xi}(t)^T \delta\dot{\xi}(t) - C_{\xi} \delta\xi(t)^T \delta\xi(t), \tag{18}$$

for some constants $C_{\xi} > 0$ and $C_{\xi} > 0$. The computation of this bound is involved, and including it here introduces a tremendous amount of complexity which may muddle the proof of the lemma at first pass. However, it is also not trivial to conclude, and hence its detailed derivation can be found in the ‘‘Appendix.’’

We now turn our attention to the potential term, $V(R(\xi(t)))$. Since V and $R(\cdot)$ are both smooth we know that the second partial derivatives of $V(R(\cdot))$ are bounded, and since V does not depend on $\dot{\xi}(t)$,

$$\nabla^2 V(R(\eta(t))) [(\delta\xi(t), \delta\dot{\xi}(t))] [(\delta\xi(t), \delta\dot{\xi}(t))] \leq C_V \delta\xi(t)^T \delta\xi(t) \tag{19}$$

for a constant C_V . Thus, combining (18) and (19), we can bound $\nabla^2\mathbb{S}_d$,

$$\begin{aligned} & \nabla^2 \mathbb{S}_d(\eta(t), \dot{\eta}(t)) [(\delta \xi(t), \delta \dot{\xi}(t))] [(\delta \xi(t), \delta \dot{\xi}(t))] \\ & \geq h \sum_{j=1}^m b_j C_{\xi} \delta \dot{\xi}(c_j h)^T \delta \dot{\xi}(c_j h) - (C_{\xi} + C_V) \delta \xi(c_j h)^T \delta \xi(c_j h). \end{aligned}$$

Since, by assumption, $\delta \xi(t)$ and $\delta \dot{\xi}(t)$ are polynomials of degree at most $n + 1$, $\delta \xi(t)^T \delta \xi(t)$ and $\delta \dot{\xi}(t)^T \delta \dot{\xi}(t)$ is a polynomial of degree at most $2n + 2$, so the quadrature rule is exact, and thus

$$\begin{aligned} & h \sum_{j=1}^m b_j C_{\xi} \delta \dot{\xi}(c_j h)^T \delta \dot{\xi}(c_j h) - (C_{\xi} + C_V) \delta \xi(c_j h)^T \delta \xi(c_j h) \\ & = C_{\xi} \int_0^h \delta \dot{\xi}(t)^T \delta \dot{\xi}(t) dt - (C_{\xi} + C_V) \int_0^h \delta \xi(t)^T \delta \xi(t) dt. \end{aligned} \tag{20}$$

$\delta \xi(t) \in H_0^1([0, h], \mathbb{R}^3)$, so we can apply the Poincaré inequality to see

$$\begin{aligned} & C_{\xi} \int_0^h \delta \dot{\xi}(t)^T \delta \dot{\xi}(t) dt - (C_{\xi} + C_V) \int_0^h \delta \xi(t)^T \delta \xi(t) dt \\ & \geq \frac{C_{\xi} \pi}{h^2} \int_0^h \delta \xi(t)^T \delta \xi(t) dt - (C_{\xi} + C_V) \int_0^h \delta \xi(t)^T \delta \xi(t) dt \\ & = \left(\frac{C_{\xi} \pi}{h^2} - (C_{\xi} + C_V) \right) \int_0^h \xi(t)^T \xi(t) dt \end{aligned}$$

which is positive so long as $h < \sqrt{\frac{C_{\xi} \pi}{C_{\xi} + C_V}}$. Thus, given that $h < \sqrt{\frac{C_{\xi} \pi}{C_{\xi} + C_V}}$, for arbitrary $(\delta \xi(t), \delta \dot{\xi}(t))$

$$\mathbb{S}_d(\check{\xi}(t) + \delta \xi(t), \dot{\check{\xi}}(t) + \delta \dot{\xi}(t)) - \mathbb{S}_d(\check{\xi}(t), \dot{\check{\xi}}(t)) > 0$$

which demonstrates that $(\check{\xi}(t), \dot{\check{\xi}}(t))$ minimizes the action. □

It should be noted that the only use of the assumption that the approximation space is polynomials of order at least n is when we use the order of the quadrature rule to change the quadrature to the exact integral (20). Thus, this proof can easily be generalized to other approximation spaces, so long as the quadrature rule used is exact for the product of any two elements of the approximation space and the product of any two derivatives of the elements of the approximation space.

3.3 Convergence of Galerkin Curves

Lie group Galerkin variational integrators require the construction of a curve

$$\tilde{g}_n(t) \in \mathbb{GM}^n(g_k \times [0, h], G)$$

such that

$$\tilde{g}_n(t) = \underset{\substack{g_n \in \text{GM}^n(g_k \times [0, h], G) \\ g_n(0) = g_k, g_n(h) = g_{k+1}}}{\text{argext}} \sum_{j=1}^m b_j L(g_n(c_j h), \dot{g}_n(c_j h)).$$

This curve, which we shall refer to as the *Galerkin curve*, is a finite-dimension approximation to the true solution of the Euler–Lagrange equations over the interval $[0, h]$. For the one-step map, we are only concerned with the right endpoint of the Galerkin curve, as

$$g_{k+1} = g_n(h).$$

However, the curve itself has excellent approximation properties as a continuous approximation to the solution of the Euler–Lagrange equations over the interior of the interval $[0, h]$. Because Lie group Galerkin variational integrators are capable of taking very large time-steps, the dynamics during the interior of these time-steps may be of interest, and hence the quality of the approximation by these Galerkin curves is also of particular interest. For example, see the numerical simulation of the three-dimensional pendulum in Sect. 5, where the dynamics of the pendulum on the interior of the time-step are sophisticated and interesting in their own right.

Ideally, these curves would have the same order of error as the one-step map. Unfortunately, we can only establish error estimates with lower orders of approximation. We established similar results in the vector space case, see Hall and Leok [13], and observed that at high enough accuracy, there is indeed greater error in the Galerkin curve than the one-step map. However, when comparing these curves to the true solution, typically the error introduced by the inaccuracies in (g_k, g_{k+1}) dominates the error from the Galerkin curve, and thus this lower rate of convergence was not observed in practice.

Before we formally establish the rates of convergence for the Galerkin curves, we will briefly review the norms we will use in our theorems and proofs. First, recall the L_p norm for functions over the interval $[0, h]$ given by

$$\|f\|_{L^p([0, h])} = \left(\int_0^h |f|^p dt \right)^{\frac{1}{p}}$$

and next, the Sobolev norm $\|\cdot\|_{W^{1,p}([0, h])}$ for functions on the interval $[0, h]$, given by:

$$\|f\|_{W^{1,p}([0, h])} = \left(\|f\|_{L^p([0, h])}^p + \|\dot{f}\|_{L^p([0, h])}^p \right)^{\frac{1}{p}}.$$

Also, note that for curves $\xi(t) \in \mathfrak{g}$, $|\xi(t)| = \langle \xi(t), \xi(t) \rangle^{\frac{1}{2}}$. We will make extensive use of these definitions in the next three theorems.

We first present an error theorem which bounds the error in the Galerkin curve, subject to conditions on the action. Again, while the notation for the theorem may be

slightly cumbersome, the idea is relatively straightforward: If the action is sufficiently well behaved (we will define this more precisely in the statement of the theorem), then

- (1) the bound on the difference between the exact discrete Lagrangian and the Lie group Galerkin discrete Lagrangian can be used to bound the difference of the value of the action evaluated on the true solution and the value of the action evaluated on the Galerkin curve, which in turn
- (2) can be used to bound the error of the Galerkin curve.

In this way, we use the error of the one-step map to bound the error of the Galerkin curve.

Theorem 3.3 *Under the same assumptions as Theorem 3.2, consider the action as a function of the local left trivialization of the Lie group curve and its derivative,*

$$\mathfrak{S}_{\mathfrak{g}}(\bar{\eta}(t), \dot{\bar{\eta}}(t)) = \int_0^h L\left(L_{\mathfrak{g}}\Phi(\bar{\eta}(t)), \frac{d}{dt}L_{\mathfrak{g}}\Phi(\bar{\eta}(t))\right) dt,$$

where $L_{\mathfrak{g}}\Phi(\bar{\eta}(t))$ satisfies the Euler–Lagrange equations exactly. If at $(\bar{\eta}(t), \dot{\bar{\eta}}(t))$ the action $\mathfrak{S}_{\mathfrak{g}}(\cdot, \cdot)$ is twice Frechet differentiable and the second Frechet derivative is coercive in variations of the Lie algebra, that is,

$$\left|D^2\mathfrak{S}_{\mathfrak{g}}((\bar{\eta}(t), \dot{\bar{\eta}}(t)))[(\delta\xi(t), \delta\dot{\xi}(t))][(\delta\xi(t), \delta\dot{\xi}(t))]\right| \geq C_f \|\delta\xi(t)\|_{W^{1,1}([0,h])}^2$$

for all $\delta\xi(t) \in H_0^1([0, h], \mathfrak{g})$, then if the one-step map has error $\mathcal{O}(K^n)$, the Galerkin curves have error $\mathcal{O}(\sqrt{K^n})$ in Sobolev norm $\|\cdot\|_{W^{1,1}([0,h])}$.

Proof We start with the bound (33), given at the end of the proof of Theorem 3.2 in the “Appendix,”

$$\left|L_d^E(g_k, g_{k+1}, h) - L_d^G(g_k, g_{k+1}, n)\right| \leq C_s K_s^n,$$

expand using the definitions of $L_d^E(g_k, g_{k+1}, h)$ and $L_d^G(g_k, g_{k+1}, n)$, and using the assumption on the accuracy of the quadrature rule

$$\begin{aligned} C_s K_s^n &\geq \left|L_d^E(g_k, g_{k+1}, h) - L_d^G(g_k, g_{k+1}, n)\right| \\ &\geq \left|\int_0^h L\left(L_{g_k}\Phi(\bar{\eta}(t)), \frac{d}{dt}L_{g_k}\Phi(\bar{\eta}(t))\right) dt \right. \\ &\quad \left. - \sum_{j=1}^m b_j L\left(L_{g_k}\Phi(\bar{\eta}(t)), \frac{d}{dt}L_{g_k}\Phi(\bar{\eta}(t))\right)\right| \\ &\geq \left|\int_0^h L\left(L_{g_k}\Phi(\bar{\eta}(t)), \frac{d}{dt}L_{g_k}\Phi(\bar{\eta}(t))\right) dt \right. \end{aligned}$$

$$\begin{aligned}
 & - \int_0^h L \left(L_{gk} \Phi (\tilde{\eta} (t)), \frac{d}{dt} L_{gk} \Phi (\tilde{\eta} (t)) \right) dt \Big| - C_g K_g^n \\
 & = \left| \mathfrak{S}_{\mathfrak{g}} (\tilde{\eta} (t), \dot{\tilde{\eta}} (t)) - \mathfrak{S}_{\mathfrak{g}} (\tilde{\eta} (t), \dot{\tilde{\eta}} (t)) \right| - C_g K_g^n.
 \end{aligned}$$

We know from the proof of Theorem 3.2 that $K_g \leq K_s$, and this implies

$$(C_s + C_g) K_s^n \geq \left| \mathfrak{S}_{\mathfrak{g}} (\tilde{\eta} (t), \dot{\tilde{\eta}} (t)) - \mathfrak{S}_{\mathfrak{g}} (\tilde{\eta} (t), \dot{\tilde{\eta}} (t)) \right|. \tag{21}$$

We now Taylor expand around the exact solution $(\tilde{\eta} (t), \dot{\tilde{\eta}} (t))$

$$\begin{aligned}
 \mathfrak{S}_{\mathfrak{g}} (\tilde{\eta} (t), \dot{\tilde{\eta}} (t)) & = \mathfrak{S}_{\mathfrak{g}} (\tilde{\eta} (t), \dot{\tilde{\eta}} (t)) + D\mathfrak{S}_{\mathfrak{g}} (\tilde{\eta} (t), \dot{\tilde{\eta}} (t)) \left[\tilde{\eta} (t) - \tilde{\eta} (t), \dot{\tilde{\eta}} (t) - \dot{\tilde{\eta}} (t) \right] \\
 & \quad + \frac{1}{2} D^2 \mathfrak{S}_{\mathfrak{g}} (\nu (t), \dot{\nu} (t)) \left[\left(\tilde{\eta} (t) - \tilde{\eta} (t), \dot{\tilde{\eta}} (t) - \dot{\tilde{\eta}} (t) \right) \right] \\
 & \quad \left[\left(\tilde{\eta} (t) - \tilde{\eta} (t), \dot{\tilde{\eta}} (t) - \dot{\tilde{\eta}} (t) \right) \right], \tag{22}
 \end{aligned}$$

where $\nu (t)$ is a curve in \mathfrak{g} . Now, note that $D\mathfrak{S}_{\mathfrak{g}} (\tilde{\eta} (t), \dot{\tilde{\eta}} (t)) = 0$ is exactly the stationarity condition of the Euler–Lagrange equations. Thus, inserting (22) into (21) yields

$$\begin{aligned}
 (C_s + C_g) K_s^n & \geq \frac{1}{2} \left| D^2 \mathfrak{S}_{\mathfrak{g}} (\nu (t), \dot{\nu} (t)) \left[\left(\tilde{\eta} (t) - \tilde{\eta} (t), \dot{\tilde{\eta}} (t) - \dot{\tilde{\eta}} (t) \right) \right] \right. \\
 & \quad \left. \left[\left(\tilde{\eta} (t) - \tilde{\eta} (t), \dot{\tilde{\eta}} (t) - \dot{\tilde{\eta}} (t) \right) \right] \right| \\
 & \geq \frac{C_f}{2} \|\tilde{\eta} (t) - \tilde{\eta} (t)\|_{W^{1,1}([0,h])}^2 \tag{23}
 \end{aligned}$$

where we have made use of the coercivity of the second derivative of the action. Simplifying (23) yields

$$\sqrt{\frac{2(C_s + C_g)}{C_f}} \sqrt{K_s^n} \geq \|\tilde{\eta} (t) - \tilde{\eta} (t)\|_{W^{1,1}([0,h])},$$

which establishes convergence in the Sobolev norm. □

Just as we proved a theorem about arbitrarily high-order convergence, Theorem 3.1, that was analogous to the geometric convergence theorem, Theorem 3.2, we can establish an analogous convergence theorem for Galerkin curves with h -refinement.

Theorem 3.4 *Under the same assumptions as Theorem 3.1, consider the action as a function of the local left trivialization of the Lie group curve and its derivative,*

$$\mathfrak{S}_{\mathfrak{g}} (\tilde{\eta}, \dot{\tilde{\eta}}) = \int_0^h L \left(L_g \Phi (\tilde{\eta}), \frac{d}{dt} L_g \Phi (\tilde{\eta}) \right) dt.$$

If at $(\bar{\eta}, \dot{\bar{\eta}})$ the action $\mathfrak{S}_{\mathfrak{g}}(\cdot, \cdot)$ is twice Frechet differentiable and the second Frechet derivative is coercive in variations of the Lie algebra as in Theorem 3.3, then if the one-step map has error $\mathcal{O}(h^{n+1})$, then the Galerkin curves have error $\mathcal{O}\left(h^{\frac{n+1}{2}}\right)$ in the Sobolev norm $\|\cdot\|_{W^{1,1}([0,h])}$.

The proof Theorem 3.4 is nearly identical to that of Theorem 3.3, the only difference being that the bounds containing K_s^n are replaced with bounds containing h^{n+1} in the obvious way.

Like the assumption that the stationary point of the discrete action is a minimizer in Theorems 3.2 and 3.1, the assumption that the second Frechet derivative of the action is coercive might seem quite strong. However, we can show that for Lagrangians on $SO(3)$ of the form

$$L(R, \dot{R}) = \text{tr}\left(\dot{R}^T R J_d R^T \dot{R}\right) - V(R),$$

the second Frechet derivative of the action is coercive, subject to a time-step restriction on h .

Lemma 3.2 *For Lagrangians on $SO(3)$ of the form*

$$L(R, \dot{R}) = \text{tr}\left(\dot{R}^T R J_d R^T \dot{R}\right) - V(R),$$

there exists a $C > 0$ such that for $h < C$, the second Frechet derivative of $\mathfrak{S}_{\mathfrak{g}}(\cdot, \cdot)$ at $(\bar{\eta}(t), \dot{\bar{\eta}}(t))$ is coercive on the interval $[0, h]$.

The proof of this theorem is similar in spirit to the proof that the stationary points of the actions are minimizers, Lemma 3.1, with the caveat that we now need to prove a slightly stronger result. This is achieved by leveraging much of the work of Lemma 3.1, and then carefully extending that analysis to achieve the stronger result, although at the cost of a stronger restriction on h . Again, the proof of the theorem is involved and can be daunting at first pass, and since it is conceptually similar to the proof of Lemma 3.1, we will not present it here. However, it is sufficiently distinct from the proof of Lemma 3.1 that it may be of interest in its own right, and hence it is included in the “Appendix.”

4 Cayley Transform Based Method on $SO(3)$

Because the construction of a Lie group Galerkin variational integrator can be involved, we will provide an example of an integrator based on the Cayley transform for the rigid body on $SO(3)$ and related problems. We will first construct the method and then verify that it satisfies the hypotheses of Theorems 3.1 and 3.2, and in Sect. 5 we will demonstrate numerically that it exhibits the expected convergence.

Additionally, discretizing the rigid body amounts to discretizing a kinetic energy term that can be used in many different applications. It appears that discretizing the kinetic energy term of the rigid body is more painstaking than the potential term, so

we provide a detailed description so that others will not have to repeat the derivation of this discretization for future applications.

4.1 Rigid Body on $SO(3)$

The Lagrangian:

$$L(R, \dot{R}) = \text{tr} \left(\dot{R}^T R J_d R^T \dot{R} \right) \tag{24}$$

$$\begin{aligned} J_d &= \frac{1}{2} \text{tr} [J] I_{3 \times 3} - J \\ J &= \text{tr} [J_d] I_{3 \times 3} - J_d, \end{aligned} \tag{25}$$

where $R \in SO(3)$ and J is the moments of inertia in the reference coordinate frame, gives rise to the equations of motion for the rigid body. The rigid body has a rich geometric structure, which is discussed in Lee et al. [20,21], Celledoni and Owren [8], and Marsden and Ratiu [27]. In addition to being an interesting example of a non-canonical Lagrangian system, it is a standard model problem for discretization for numerical methods on Lie groups, and an overview of integrators applied to the rigid body can be found in Hairer et al. [12].

4.2 Construction

To construct the Lie group Galerkin variational integrator, we will have to choose:

- (1) a map $\Phi(\cdot) : \mathfrak{so}(3) \rightarrow SO(3)$,
- (2) a finite-dimensional function space $\mathbb{M}^n([0, h], \mathfrak{g})$, and
- (3) a quadrature rule,

and to complete the error analysis, we must also choose

- (1) a metric on $\mathfrak{so}(3)$ $\langle \cdot, \cdot \rangle$,
- (2) error functions $e_g(\cdot, \cdot)$ and $e_a(\cdot, \cdot)$.

For our construction, we will make use of the Cayley transform for our map $\Phi(\cdot)$, Lagrange interpolation polynomials through $\mathfrak{so}(3)$ for the finite-dimensional function space $\mathbb{M}^n([0, h], \mathfrak{g})$, that is,

$$\mathbb{M}^n([0, h], \mathfrak{g}) = \left\{ \xi(t) \mid \xi(t) = \sum_{i=1}^n q^i \widehat{\phi_i}(t), q^i \in \mathbb{R}^3, \phi_i(t) \right. \\ \left. \text{is the Lagrange interpolation polynomial for } t_i \right\},$$

where $\hat{\cdot}$ is that hat map defined by (17), and high-order Gauss–Legendre quadrature for our quadrature rule. For the error analysis we will choose:

$$\langle \hat{\eta}, \hat{v} \rangle = \eta^T v,$$

$$e_g(G_1, G_2) = \|G_1 - G_2\|_2$$

$$e_a(\hat{\eta}, \hat{v}) = \|\hat{\eta} - \hat{v}\|_2,$$

for arbitrary $G_1, G_2 \in SO(3)$ and $\eta, v \in \mathbb{R}^3$, where the $\|\cdot\|_2$ norm is understood as arising from the $\|\cdot\|_2$ norm from the embedding space $\mathbb{R}^{3 \times 3}$. We will discuss these below, and elaborate on the motivation for these choices in our construction.

4.2.1 The Cayley Transform

To construct our Lie group Galerkin variational Integrator, we will make use of the Cayley transform, $\Phi(\cdot) : \mathfrak{so}(3) \rightarrow SO(3)$ which is given by:

$$\Phi(q) = (I - Q)(I + Q)^{-1}.$$

The reader should note that we are using an unscaled version of the Cayley transform, but for the purposes of constructing the natural chart, different versions of the Cayley transform should result in equivalent methods. Furthermore, utilizing the Cayley transform to construct the integrator is certainly not the only valid option; different choices of maps, such as the exponential map, would result in equally valid methods. We make use of the Cayley transform simply because it is easy to manipulate and compute, is its own inverse, and because it satisfies our chart conditioning assumptions, as we will establish shortly.

Lemma 4.1 For $\eta, v \in \mathfrak{so}(3)$, so long as

$$2\|\eta\|_2 + \|v\|_2 < 1, \tag{26}$$

the natural chart constructed by the Cayley transform locally satisfies chart conditioning assumption, that is:

$$\|\Phi(\eta) - \Phi(v)\|_2 \leq C_G \langle \eta - v, \eta - v \rangle^{\frac{1}{2}}$$

$$\|D_\eta \Phi(\dot{\eta}) - D_v \Phi(\dot{v})\|_2 \leq C_g \langle \eta - v, \eta - v \rangle^{\frac{1}{2}} + C_g^G \langle \dot{\eta} - \dot{v}, \dot{\eta} - \dot{v} \rangle^{\frac{1}{2}}.$$

If $\|\eta - v\|_2 < \epsilon$, assumption (26) can be relaxed to

$$\|\eta\|_2 + \epsilon < 1.$$

The proof of this lemma amounts to a very long sequence of matrix inequalities, and again for brevity and clarity’s sake we shall not include it here; it can be found in the “Appendix.” It should be noted that as $\|v\|_2$ or $\|\eta\|_2$ approaches 1, C_G, C_g and C_g^G increase without bound. This amounts to a time-step restriction for the method; if the configuration changes too dramatically during the time-step, the chart will become poorly conditioned and the numerical solution will degrade. However, as long as $\|v\|_2 < C_{con}$ and $\|\eta\|_2 < C_{con}$ on each time-step for some $C_{con} < 1$ which is independent of the number of the time-step, these constants will remain bounded and the natural chart will be well conditioned.

4.2.2 Choice of Basis Functions

The second feature of the construction of our Cayley transform Lie group Galerkin variational integrator is the choice of function space $\mathbb{M}^n ([0, h], \mathfrak{g})$ for approximation of curves in the Lie algebra. Since the curves in the Lie algebra $\mathfrak{so}(3)$ that we use have a natural correspondence with curves in \mathbb{R}^3 through the hat map, constructing these curves reduces to choosing an approximation space for curves in \mathbb{R}^3 .

We make the choice of polynomials of degree at most n for $\mathbb{M}^n ([0, h], \mathfrak{g})$. We choose polynomials because approximation theory and particularly the theory of spectral numerical methods, see Trefethen [38], tells us that polynomials have excellent convergence under both h and n refinement to smooth curves, and in particular, analytic curves. For the basis functions $\{\phi_i(t)\}_{i=1}^n$, we choose $\phi_i(t)$ to be the Lagrange interpolation polynomial for the i -th of n Chebyshev points rescaled to the interval $[0, h]$, that is

$$\phi_i(t) = \frac{\prod_{j=1, j \neq i}^n (t - t_j)}{\prod_{j=1, j \neq i}^n (t_i - t_j)}$$

for $t_i = \frac{h}{2} \cos\left(\frac{i\pi}{n}\right) + \frac{h}{2}$. While our convergence theory does not depend on the choice of polynomial basis, there are two major benefits for this choice of basis functions. The first is that these polynomials interpolate 0 and h , which greatly simplifies the computation of the discrete Legendre transforms $D_1L_d(R_k, R_{k+1})$ and $D_2L_d(R_{k-1}, R_k)$. The second is that this choice of basis function results in methods which have internal stage equations that are more numerically stable in practice than other choices of interpolation points, most likely because of the excellent stability properties of the interpolation polynomials that are constructed from them. The interested reader is referred to Trefethen [38] and Boyd [6] and the references therein for more details on spectral numerical methods.

4.2.3 Choice of Quadrature Rule

The final selection we must make when constructing the integrator is a choice of quadrature rule. We choose to use Gaussian quadrature, mostly because this quadrature rule is optimally accurate in the number of points and because it is simple to compute higher-order Gaussian quadrature points and weights by solving a small eigenvalue problem. However, it is possible to use other rules, and we make no claim that our choice is the best for our choice of parameters.

4.3 Discrete Euler–Lagrange Equations

While in Sect. 2.2.3 we presented a general form of the internal stage discrete Euler–Lagrange equations in coordinate-free notation, direct construction of these equations is probably not the easiest way to formulate a numerical method. This is because it requires the computation and composition of many different functions, some of which may be complicated (for example, working out $\mathbf{D}_{\alpha, \dot{\alpha}} \mathbf{D}_\alpha \Phi(\mathbf{D}_{q_i} \alpha, \mathbf{D}_{\dot{q}_i} \dot{\alpha})$ for the Cayley

transform is straightforward, but also slightly obnoxious). An alternative approach, to which we alluded in Sect. 2.2.3, is to compute the discrete action in coordinates, and then explicitly compute the stationarity conditions for this discrete action. We do this here for the rigid body equations.

For the construction of the Lie group Galerkin variational integrator for the rigid body, we make use of the following functions:

$$\begin{aligned}
 R_n \left(\left\{ \xi^i \right\}_{i=1}^n, t \right) &= R_k \Phi \left(\sum_{i=1}^n \hat{\xi}^i \phi_i(t) \right) \\
 L(R(t), \dot{R}(t)) &= \text{tr} \left(\dot{R}(t)^T R(t) J_d R(t)^T \dot{R}(t) \right) \\
 L_d(R_k, R_{k+1}) &= \underset{\substack{R_n \in \mathbb{G}\mathbb{M}^n(R_k \times [0, h], G) \\ R_n(0) = R_k, R_n(h) = R_{k+1}}}{\text{ext}} h \sum_{j=1}^m b_j L(R_n(c_j h), \dot{R}_n(c_j h)) \quad (27)
 \end{aligned}$$

where $\xi^i \in \mathbb{R}^3$. Since the curve $R_n(t)$ is a function on n points in \mathbb{R}^3 , denoting $\xi^i = (\xi_a^i, \xi_b^i, \xi_c^i)$, we can write (27) as

$$\begin{aligned}
 L_d(R_k, R_{k+1}) &= \underset{\xi^0=0, \xi^n=\Phi^{-1}(R_k^T R_{k+1})}{\text{ext}} h \sum_{j=1}^m b_j \frac{2}{\left(1 + \|\xi(c_j h)\|_2^2\right)^2} \left(I_1 \varphi(\xi_c, \xi_a, \xi_b)^2 \right. \\
 &\quad \left. + I_2 \varphi(\xi_b, \xi_c, \xi_a)^2 + I_3 \varphi(\xi_a, \xi_b, \xi_c)^2 \right)
 \end{aligned}$$

where

$$\varphi(\xi_a, \xi_b, \xi_c) = \dot{\xi}_a(c_j h) + \xi_b(c_j h) \dot{\xi}_c(c_j h) - \xi_c(c_j h) \dot{\xi}_b(c_j h),$$

$\varphi(\xi_c, \xi_a, \xi_b)$ and $\varphi(\xi_b, \xi_c, \xi_a)$ are defined analogously, and

$$\begin{aligned}
 I_i &= \sum_{j \neq i} (J_d)_{jj} \\
 \xi_x(t) &= \sum_i^n \xi_x^i \phi_i(t) \\
 \xi(t) &= (\xi_a(t), \xi_b(t), \xi_c(t)).
 \end{aligned}$$

Forming the action sum as a function of the ξ^i ,

$$\begin{aligned}
 \mathbb{S}_d \left(\left\{ \xi^i \right\}_{i=1}^n \right) &= h \sum_{j=1}^m b_j \frac{2}{\left(1 + \|\xi(c_j h)\|_2^2\right)^2} \\
 &\quad \left(I_1 \varphi(\xi_c, \xi_a, \xi_b)^2 + I_2 \varphi(\xi_b, \xi_c, \xi_a)^2 + I_3 \varphi(\xi_a, \xi_b, \xi_c)^2 \right)
 \end{aligned}$$

computing its variational derivative from ξ^i directly and setting it equal to 0,

$$\frac{d}{d\epsilon} \mathbb{S}_d \left(\left\{ \xi^i + \epsilon \delta \xi^i \right\}_{i=1}^n \right) \Big|_{\epsilon=0} = 0,$$

gives the internal stage discrete Euler–Lagrange equations,

$$\begin{aligned} & h \sum_{j=1}^m b_j 4 \left(1 + \|\xi\|_2^2 \right)^{-2} \left[(I_3 \varphi (\xi_c, \xi_a, \xi_b)) \right. \\ & \quad \left(-2 \left(1 + \|\xi\|_2^2 \right)^{-1} \varphi (\xi_c, \xi_a, \xi_b) \xi_a \phi_i + \dot{\xi}_b \phi_i - \xi_b \dot{\phi}_i \right) \\ & \quad + (I_2 \varphi (\xi_b, \xi_c, \xi_a)) \left(-2 \left(1 + \|\xi\|_2^2 \right)^{-1} \varphi (\xi_b, \xi_c, \xi_a) \xi_a \phi_i + \xi_c \dot{\phi}_i - \dot{\xi}_c \phi_i \right) \\ & \quad \left. + (I_1 \varphi (\xi_a, \xi_b, \xi_c)) \left(-2 \left(1 + \|\xi\|_2^2 \right)^{-1} \varphi (\xi_a, \xi_b, \xi_c) \xi_a \phi_i + \dot{\phi}_i \right) \right] = 0 \end{aligned} \tag{28a}$$

$$\begin{aligned} & h \sum_{j=1}^m b_j 4 \left(1 + \|\xi\|_2^2 \right)^{-2} \left[(I_3 \varphi (\xi_c, \xi_a, \xi_b)) \right. \\ & \quad \left(-2 \left(1 + \|\xi\|_2^2 \right)^{-1} \varphi (\xi_c, \xi_a, \xi_b) \xi_b \phi_i + \xi_a \dot{\phi}_i - \dot{\xi}_a \phi_i \right) \\ & \quad + (I_2 \varphi (\xi_b, \xi_c, \xi_a)) \left(-2 \left(1 + \|\xi\|_2^2 \right)^{-1} \varphi (\xi_b, \xi_c, \xi_a) \xi_b \phi_i + \dot{\phi}_i \right) \\ & \quad \left. + (I_1 \varphi (\xi_a, \xi_b, \xi_c)) \left(-2 \left(1 + \|\xi\|_2^2 \right)^{-1} \varphi (\xi_a, \xi_b, \xi_c) \xi_b \phi_i + \dot{\xi}_c \phi_i - \xi_c \dot{\phi}_i \right) \right] = 0 \end{aligned} \tag{28b}$$

$$\begin{aligned} & h \sum_{j=1}^m b_j 4 \left(1 + \|\xi\|_2^2 \right)^{-2} \left[(I_3 \varphi (\xi_c, \xi_a, \xi_b)) \left(-2 \left(1 + \|\xi\|_2^2 \right)^{-1} \varphi (\xi_c, \xi_a, \xi_b) \xi_c \phi_i + \dot{\phi}_i \right) \right. \\ & \quad + (I_2 \varphi (\xi_b, \xi_c, \xi_a)) \left(-2 \left(1 + \|\xi\|_2^2 \right)^{-1} \varphi (\xi_b, \xi_c, \xi_a) \xi_c \phi_i + \dot{\xi}_a \phi_i - \xi_a \dot{\phi}_i \right) \\ & \quad \left. + (I_1 \varphi (\xi_a, \xi_b, \xi_c)) \left(-2 \left(1 + \|\xi\|_2^2 \right)^{-1} \varphi (\xi_a, \xi_b, \xi_c) \xi_c \phi_i + \xi_b \dot{\phi}_i - \dot{\xi}_b \phi_i \right) \right] = 0, \end{aligned} \tag{28c}$$

for $i = 2, \dots, n - 1$, and where we have suppressed the t argument on all of our functions. Solving these equations, along with the condition $\xi^1 = 0$ and the discrete Euler–Lagrange equations

$$D_1 L_d (R_k, R_{k+1}) + D_2 L_d (R_{k-1}, R_k) = 0, \tag{29}$$

which we will discuss in Sect. 4.3.1, yields $\tilde{R}(t)$, the stationary point of the discrete action. Using this stationary point, computing $\tilde{R}(h) = R_{k+1}$ gives us the next step of our one-step map.

4.3.1 Momentum Matching

As we mentioned in our general derivation of the discrete Euler–Lagrange equations, (29) must be treated with care. We described in Sect. 2 an expedient method for computing $D_1 L_d(R_k, R_{k+1})$ so that the result is compatible with our change of natural charts. We will provide an explicit example below.

We already know the expression for $D_1 L_d(R_k, R_{k+1})$ for the coordinates in the current natural chart, the vector of the form (28a)–(28c), with $i = 1$. This is the map $\frac{\partial L_d}{\partial \xi_k}$ described in Sect. 2.2.4. Now, we need to compute an expression for λ_k and $\frac{\partial \xi_k}{\partial \lambda_k}$. Given $\xi_0 = (\xi_a^0, \xi_b^0, \xi_c^0)$ and $\xi_k = (\xi_a, \xi_b, \xi_c)$, we compute λ by

$$\hat{\lambda} = \Phi^{-1} \left(\Phi \left(\hat{\xi}_0 \right) \Phi \left(\hat{\xi}_k \right) \right)$$

which gives in coordinates $\lambda = (\lambda_a, \lambda_b, \lambda_c)$,

$$\begin{aligned} \lambda_a &= \frac{-\xi_a - \xi_a^0 + \xi_c \xi_b^0 - \xi_b \xi_c^0}{-1 + \xi_a^0 \xi_a + \xi_b^0 \xi_b + \xi_c^0 \xi_c} \\ \lambda_b &= \frac{-\xi_b - \xi_b^0 + \xi_a \xi_c^0 - \xi_c \xi_a^0}{-1 + \xi_a^0 \xi_a + \xi_b^0 \xi_b + \xi_c^0 \xi_c} \\ \lambda_c &= \frac{-\xi_c - \xi_c^0 + \xi_b \xi_a^0 - \xi_a \xi_b^0}{-1 + \xi_a^0 \xi_a + \xi_b^0 \xi_b + \xi_c^0 \xi_c}. \end{aligned}$$

Now, we recompute ξ_k in terms of λ ,

$$\hat{\xi}_k = \Phi^{-1} \left(\left(\Phi \left(\hat{\xi}_0 \right) \right)^{-1} \Phi \left(\hat{\lambda} \right) \right)$$

which, when expressed in coordinates $\xi_k = (\xi_a, \xi_b, \xi_c)$, gives

$$\begin{aligned} \xi_a &= \frac{\lambda_a - \xi_a^0 + \lambda_c \xi_b^0 - \lambda_b \xi_c^0}{1 + \lambda_a \xi_a^0 + \lambda_b \xi_b^0 + \lambda_c \xi_c^0} \\ \xi_b &= \frac{\lambda_b - \xi_b^0 + \lambda_a \xi_c^0 - \lambda_c \xi_a^0}{1 + \lambda_a \xi_a^0 + \lambda_b \xi_b^0 + \lambda_c \xi_c^0} \\ \xi_c &= \frac{\lambda_c - \xi_c^0 + \lambda_b \xi_a^0 - \lambda_a \xi_b^0}{1 + \lambda_a \xi_a^0 + \lambda_b \xi_b^0 + \lambda_c \xi_c^0}. \end{aligned}$$

So, to compute $D_1 L_d (R_k, R_{k+1}) = \left(\frac{\partial L_d}{\partial \lambda_a}, \frac{\partial L_d}{\partial \lambda_b}, \frac{\partial L_d}{\partial \lambda_c} \right)$, we can take the easily computed expression $\frac{\partial L_d}{\partial \xi_k}$ and apply a change of coordinates,

$$\begin{aligned} \frac{\partial L_d}{\partial \lambda_a} &= \frac{\partial L_d}{\partial \xi_a} \frac{\partial \xi_a}{\partial \lambda_a} + \frac{\partial L_d}{\partial \xi_b} \frac{\partial \xi_b}{\partial \lambda_a} + \frac{\partial L_d}{\partial \xi_c} \frac{\partial \xi_c}{\partial \lambda_a} \\ \frac{\partial L_d}{\partial \lambda_b} &= \frac{\partial L_d}{\partial \xi_a} \frac{\partial \xi_a}{\partial \lambda_b} + \frac{\partial L_d}{\partial \xi_b} \frac{\partial \xi_b}{\partial \lambda_b} + \frac{\partial L_d}{\partial \xi_c} \frac{\partial \xi_c}{\partial \lambda_b} \\ \frac{\partial L_d}{\partial \lambda_c} &= \frac{\partial L_d}{\partial \xi_a} \frac{\partial \xi_a}{\partial \lambda_c} + \frac{\partial L_d}{\partial \xi_b} \frac{\partial \xi_b}{\partial \lambda_c} + \frac{\partial L_d}{\partial \xi_c} \frac{\partial \xi_c}{\partial \lambda_c}, \end{aligned}$$

which is the momentum matching condition expressed so that it is compatible with the change of natural charts.

5 Numerical Experiments

Thus far, we have discussed the construction of Lie group Galerkin variational integrators and established bounds on their rate of convergence. We will now turn to several numerical examples to demonstrate that our methods behave in practice as our theory predicts.

5.1 Cayley Transform Method for the Rigid Body

In Sect. 4, we discussed in great detail a specific construction of a Lie group Galerkin variational integrator for the free rigid body based on the Cayley transform and polynomial basis functions. Based on the convergence results from Theorems 3.1 and 3.2, we would expect our construction to converge geometrically with n -refinement and with high order based on the number of basis functions used with h -refinement.

Using MATLAB, we implemented the Lie group Galerkin variational integrator described in Sect. 4, using a finite-difference Newton method as a root finder. We used the parameters

$$\begin{aligned} J_d &= \text{diag} (1.3, 2.1, 1.2) \\ R(0) &= I \\ R^T(0) \dot{R}(0) &= (2.0, \widehat{-1.9}, 1.0)^T. \end{aligned}$$

To establish convergence, we first computed a numerical solution using a low-order splitting method with a very small time-step, and once we established that the Lie group Galerkin variational integrator’s solution and the splitting method’s numerical solutions agreed, we used a Lie group Galerkin variational integrator solution with $n = 25$ and $h = 0.5$ as a high-order approximation to the exact solution, and established convergence to this solution. We made this choice of parameters for our approximate exact solution because it appeared that for this choice of parameters, the residual from the nonlinear solver was the dominant source of error, and neither h nor n refinement

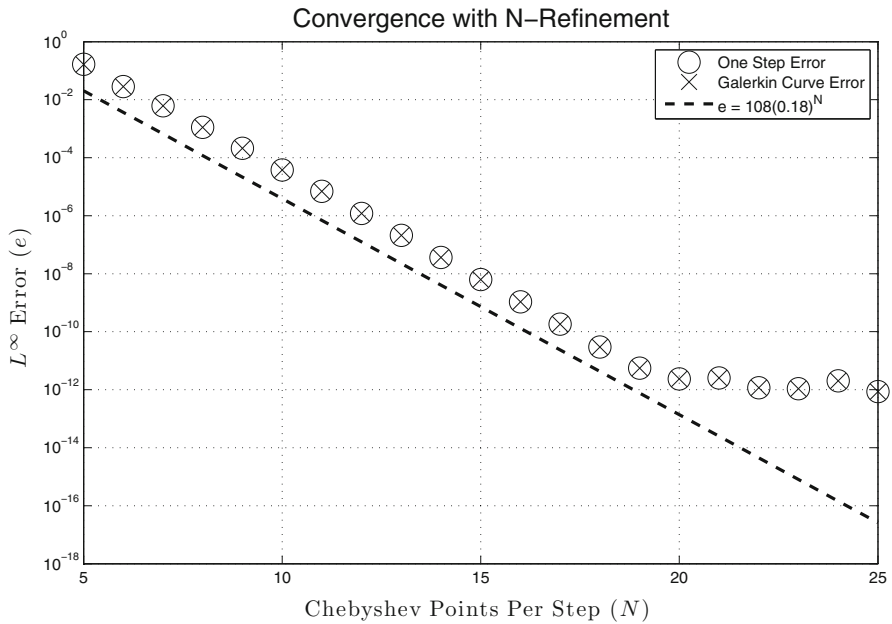


Fig. 1 Geometric convergence of the Lie group spectral variational integrator based on the Cayley transform for the rigid body. We use a constant time-step $h = 0.5$. Note that the Galerkin curves have the same error as the one-step map, even though they have a theoretical lower rate of convergence

improved our numerical solution. For all convergence experiments, we integrate to a final time of $t = 50$ and measure the absolute error at the final time.

The reader should note that, in the figures which follow, we use N to denote the number of basis functions used to create the polynomial approximation space. Thus, when interpreting the results, it is important to recall that $n = N - 1$, as the maximum degree of the polynomial in the approximation space is one less than the number of basis functions for that space. Hence, when observing convergence, our theory predicts that an integrator based on $N = 3$ basis functions, and hence $n = 2$ degree polynomials, would exhibit $O(h^2)$ convergence in the error.

The results, which are summarized in Figs. 1 and 2, establish the rates of convergence predicted in Theorems 3.1 and 3.2. With n -refinement, we see that our methods did indeed achieve geometric convergence, as can be seen in Fig. 1. However, unlike the vector space method (see Hall and Leok [13]), we did not observe the difference in convergence rates of the continuous approximation and the one-step map. We suspect that this is because until very high accuracy is achieved, the inaccurate boundary conditions due to the one-step map error dominates the continuous approximation error, and the threshold at which the continuous approximation error is greater than the one-step error is related to the time-step. While we can take extremely large time-steps with our vector space constructions, when working in Lie groups the time-step length is limited by the natural chart, and hence we never observe the lower convergence rate of the continuous approximation.

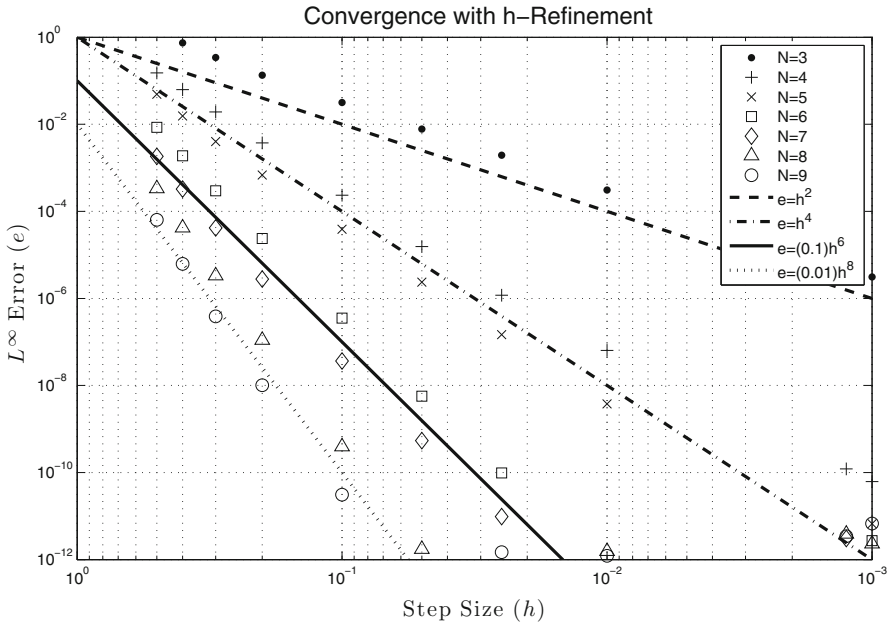


Fig. 2 Arbitrarily high-order convergence of the Lie group Galerkin variational integrator based on the Cayley transform for the rigid body. Recall that N is the number of basis functions (or Chebyshev points—these are the same) used in the construction, and hence the maximum degree of the polynomials in the approximation space is $n = N - 1$

We also examined convergence with h -refinement, as can be seen in Fig. 2. We observed the predicted rate of convergence for our constructions (recalling that $n = N - 1$), and for even N (and hence odd n), we even observed a higher than expected rate of convergence of $n + 1$.

While it is not perfectly conserved, the energy behavior of our method is oscillatory and remains bounded even for very long integration times, as can be seen in Fig. 3. This type of behavior is typical for variational integrators.

Considering the geometric invariants related to the rigid body, we see that the Cayley transform based method has excellent conservation properties. In Fig. 4, we recreate one of the classic depictions of geometric invariants for the rigid body using a Galerkin variational integrator. This figure depicts the intersection of the two hypersurfaces in momentum space given by the two geometric invariants $C(y) = \frac{1}{2} \sum_{i=1}^3 y_i^2$ and $H(y) = \frac{1}{2} \sum_{i=1}^3 I_i^{-1} y_i^2$ where y is the angular momentum of the rigid body. These invariants correspond to the norm of the body fixed angular momentum and the energy, respectively. Discussions of these invariants and comparable behavior of other methods can be found in Marsden and Ratiu [27] and Hairer et al. [12] (specifically, see Hairer et al. [12] for a comparison to other numerical methods). The black lines, which represent the evolution of the numerical trajectory of our method in momentum space from a variety of different initial conditions, remain constrained to the surface—just as they would in the true solution.

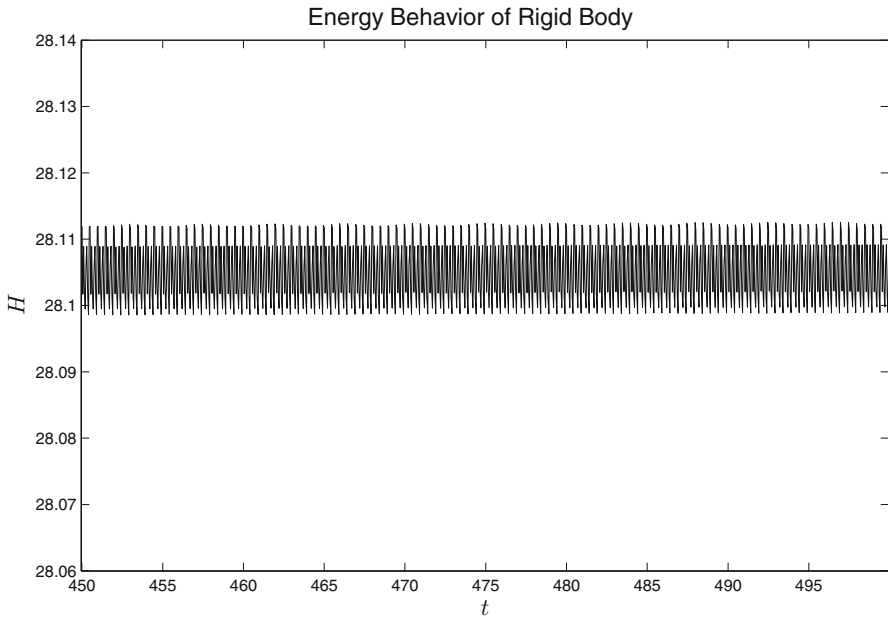


Fig. 3 Energy behavior of the Lie group Galerkin variational integrator based on the Cayley transform for the rigid body. This is from a simulation starting at $t_0 = 0.0$, and using the parameters $n = 12$, $h = 0.5$ for the integrator

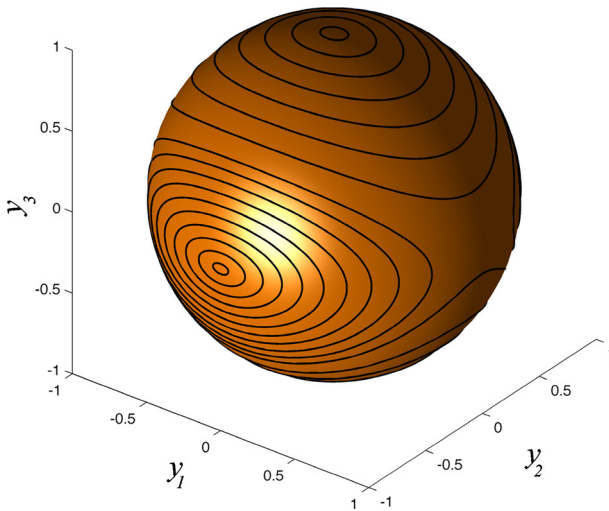


Fig. 4 Conserved quantities for the Lie group Galerkin variational integrator based on the Cayley transform for the rigid body. This is from a series of computations using the parameters $n = 8$, and $h = 0.5$, from a variety of initial conditions. Note that the trajectories computed by the Lie group Galerkin variational integrators, which are the *black curves*, lie on the intersections of $\sum_{i=1}^3 y_i^2 = 1$, $\sum_{i=1}^3 I_i^{-1} y_i^2 = 2$, which are the norm of angular momentum and energy, respectively

5.2 Cayley Transform Method for the 3D Pendulum

For a second numerical experiment, we examine the 3D pendulum. The 3D pendulum is the rigid body with one point fixed and under the influence of gravity, and its Lagrangian is:

$$L(R, \dot{R}) = \frac{1}{2} \text{tr} \left(\dot{R}^T R J_d R^T \dot{R} \right) + m g e_3^T R \rho$$

$$J_d = \text{diag} (1, 2.8, 2)$$

$$\rho = (0, 0, 1)^T$$

where ρ is center of mass for $R = I$, m is the mass of the pendulum and g is the gravitational constant. We consider two sets of initial conditions, the first,

$$\begin{aligned} R(0) &= I \\ R(0)^T \dot{R}(0) &= (0.5, \widehat{-0.5}, 0.4)^T, \end{aligned}$$

which is a slight perturbation from stable equilibrium, and the second

$$\begin{aligned} R(0) &= \text{diag} (-1, 1, -1) \\ R(0)^T \dot{R}(0) &= (0.5, \widehat{-0.5}, 0.4)^T \end{aligned}$$

which is the pendulum slightly perturbed from its unstable equilibrium.

We construct the variational integrator for this system using the Cayley transform. This involves adding the term $V(\xi(t)) = m g e_3^T L_{gk} \Phi(\xi(t)) \rho$ to the discrete action in Eq. (27), and finding the stationarity conditions of this new discrete action, which gives us the new internal stage discrete Euler–Lagrange equations. These have the same form as equations (28a)–(28c), with added terms for the potential.

For the first set of initial data, which are near the stable equilibrium, we see exactly the expected convergence with both h and n refinement, as is illustrated in Figs. 5 and 6. Furthermore, we see bounded oscillatory energy behavior over the length of the integration, as in Fig. 7. Again, we integrate to a final time of $t = 50$ and measure the absolute error at the final time.

For the second set of initial data, this system evolves chaotically, so convergence of individual trajectories is not of great interest. What is more important is the conservation of geometric invariants as the system evolves. As can be seen from Figs. 8 and 9, the energy of the system is nearly conserved, even with very aggressive time-stepping. Of particular note is that even though there are many steps where the solution undergoes a change that approaches the limit on the conditioning of the natural chart, the energy error remains small.

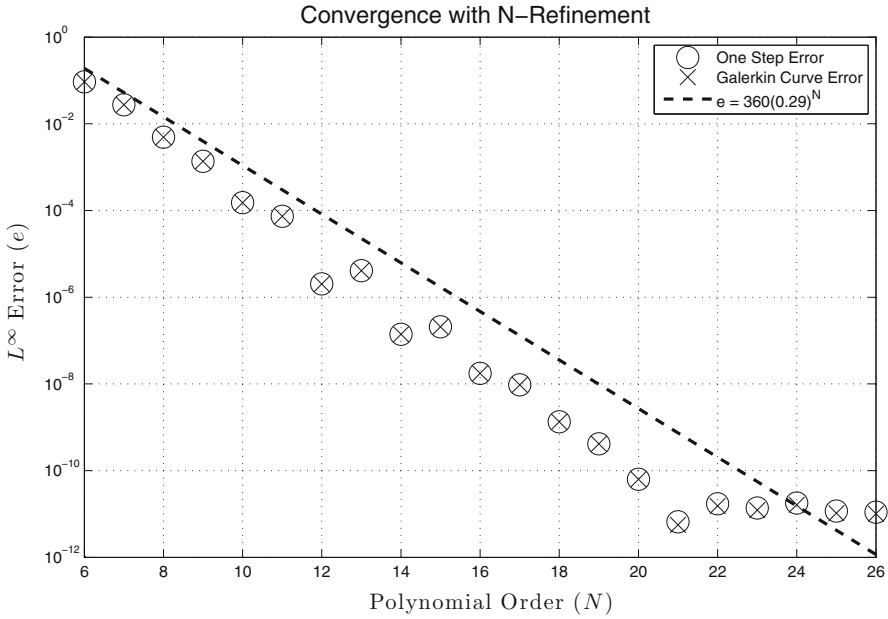


Fig. 5 Geometric convergence of the Lie group spectral variational integrator based on the Cayley transform for the 3D pendulum for a small perturbation from the stable equilibrium. We use the time-step $h = 0.5$. Note that, once again, the Galerkin curves have the same error as the one-step map

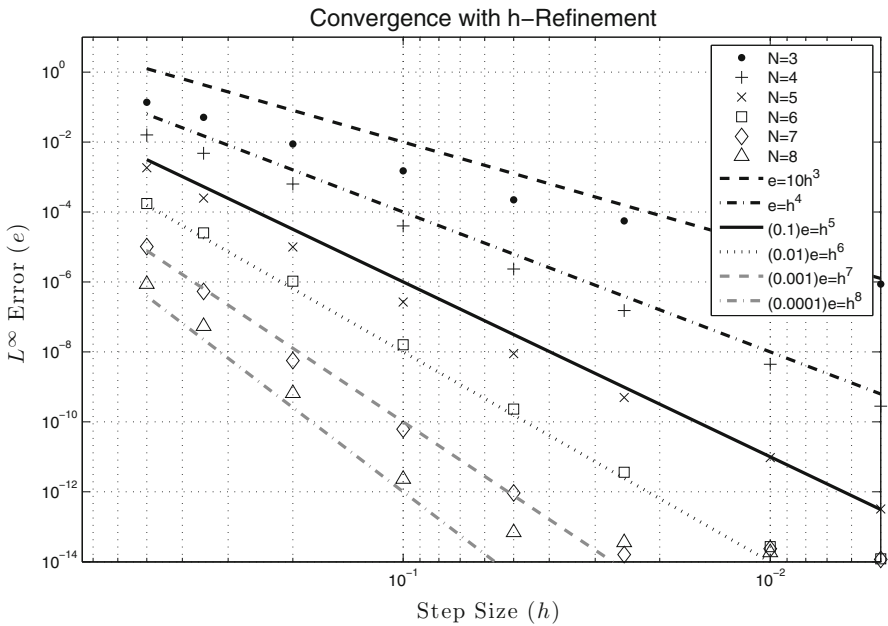


Fig. 6 High-order convergence of Lie group Galerkin variational integrator based on the Cayley transform for the 3D pendulum for a small perturbation from the stable equilibrium. Recalling that $N - 1 = n$, note that in this case, our integrators outperform our lower bound, as they exhibit $O(h^{n+1})$ convergence

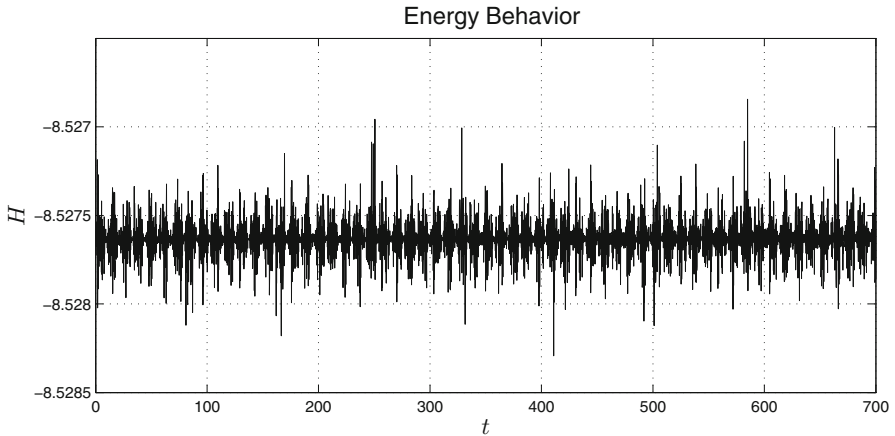


Fig. 7 Energy behavior of the Lie group Galerkin variational integrator based on the Cayley transform for the 3D pendulum for a small perturbation from the stable equilibrium. This is the behavior of an integrator constructed with parameters $n = 8$, time-step $h = 1.5$. Note that the error is both small and oscillatory, but not increasing

6 Conclusions and Future Work

In this paper, we have presented a new numerical method for Lagrangian problems on Lie groups. Specifically, we used a Galerkin construction to create variational integrators of arbitrarily high order, and also Lie group spectral variational integrators, which converge geometrically. We demonstrated that in addition to inheriting the excellent geometric properties common to all variational integrators, which include conservation of the symplectic form, and conservation of momentum, that such integrators also are extremely stable even for large time-steps, can be adapted for a large class of problems, and yield highly accurate continuous approximations to the true trajectory of the system.

We also gave an explicit example of a Lie group Galerkin variational integrator constructed using the Cayley transform. Using this construction, we demonstrated the expected rates of convergence on two different example problems, the rigid body and the 3D pendulum. We also showed that these methods both have excellent energy and momentum conservation properties. Additionally, we provided explicit expressions for the internal stage discrete Euler–Lagrange equations for the free rigid body, which form the foundation of a numerical method for a variety of problems.

6.1 Future Work

Symplectic integrators continue to be an area of interest, and there has been considerable success in developing high-order structure-preserving methods and applying such methods to relevant problems. While we have developed a significant amount of the theory of Lie group Galerkin variational integrators, there is considerable future work to be done.

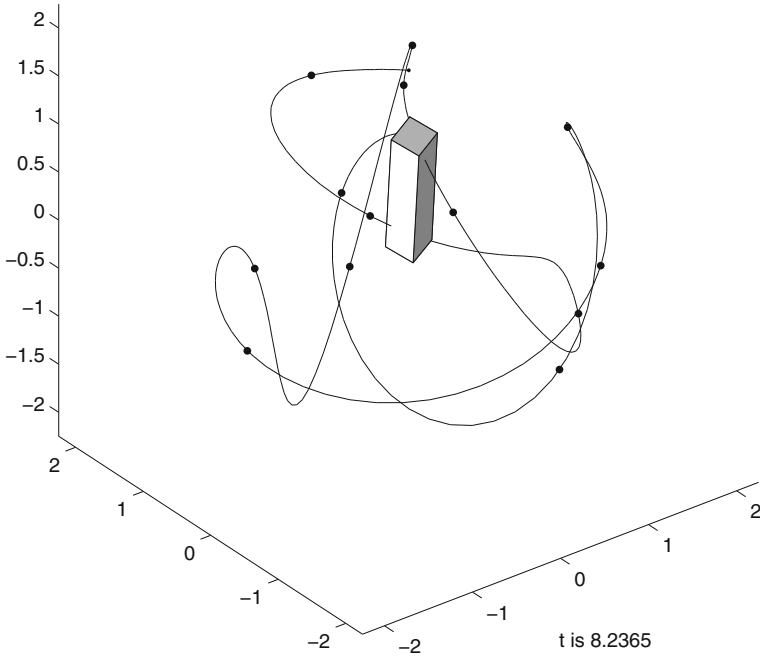


Fig. 8 Dynamics of the numerical simulation of the 3D pendulum constructed from a Lie group Galerkin variational integrator. These dynamics were constructed from an integrator with $n = 20$, $h = 0.6$. The *black dots* each represent a single step of the one-step map, and the *solid lines* are the Galerkin curves. Note that some of the steps are almost through an angle of length π , which is the limit of the conditioning of the natural chart

6.1.1 Choice of Natural Charts

In our construction, we chose the Cayley transform to construct our natural chart. While this choice made the derivation of the resulting integrator simpler, it also introduced a limitation on the conditioning of the natural chart. A possible extension of our framework would be constructions based on natural charts constructed from other functions. An obvious choice is the exponential map, which was the choice of chart function used in earlier works that proposed this construction. A comparison of the behavior of integrators constructed from other choices of natural chart functions would be interesting further work.

6.1.2 Novel Variational Integrators:

One of the attractive features of our work is that we establish an optimality result for arbitrary approximation spaces. Because of this, our results hold for a variety of

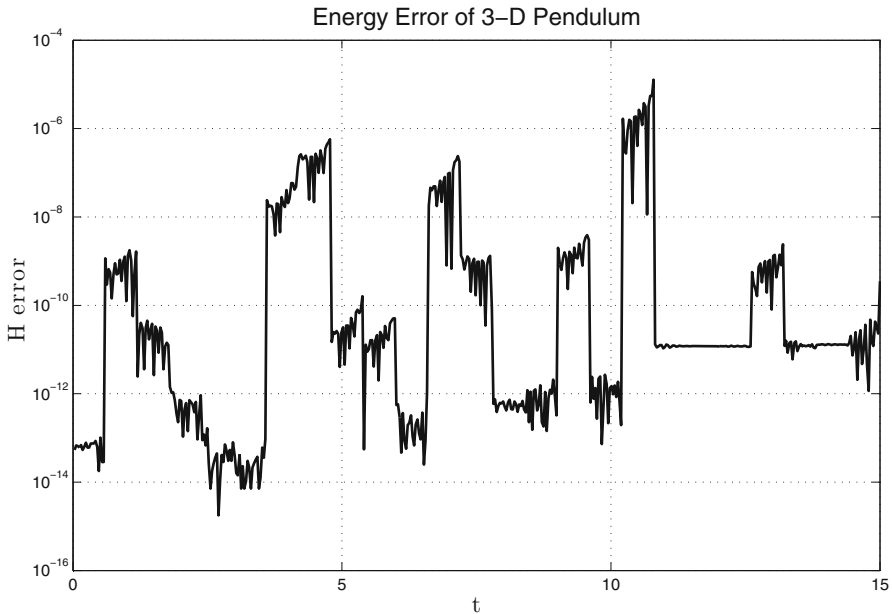


Fig. 9 Energy error of the dynamics depicted in Fig. 8. The large jumps in error are associated with time-steps that almost violate the conditioning limits of the natural chart

different possible constructions of variational integrators. It would be interesting to investigate the behavior of variational integrators constructed from novel approximation spaces, such as wavelets, or for variational integrators that make use of specialized function spaces, such as spaces that include both high and low frequency functions for problems with components that evolve on different timescales.

6.1.3 Larger classes of Problems

In this paper, we have focused most of our attention on the rigid body and problems that evolve on $SO(3)$. However, there are many examples of Lie group problems that evolve on other spaces. Our analysis suggests that the Galerkin approach would be effective for these problems. It would be interesting to examine Galerkin variational integrators for problems that evolve on other Lie groups, and apply our methods to other interesting applications.

We established the necessary estimates for convergence of a Lie group Galerkin variational integrator for Lagrangians of the form (16) and with the Cayley map. However, neither of these results rely on the fact that we are on the Lie group $SO(3)$. In particular, Lemma 3.2 for the Lagrangian will generalize to any separable Lagrangian on a matrix Lie group with a kinetic energy that is left or right invariant, and Lemma 4.1 for the Cayley map extends to any quadratic matrix group. This includes important Lie groups such as the Euclidean group $SE(3)$, the special unitary group $SU(n)$, the Lorentz group $O(1, 3)$, and the symplectic group $Sp(2n)$. Additionally, by adopting

the approach described in Section 4.2 of Lee et al. [22], Lie group Galerkin variational integrators for such matrix Lie groups could be generalized to their associated homogeneous spaces, such as the n -sphere S^n , the Stiefel manifold $V_k(\mathbb{R}^n)$, and the Grassmannian $Gr(r, n)$.

The connection between discrete variational mechanics and discrete optimal control is described in Ohsawa et al. [36], so optimal control problems on quadratic matrix groups and their associated homogeneous spaces can also be studied. These include trajectory generation problems for robotics, autonomous vehicles, variational interpolation of camera pose in computer animation problems, and optimal pulse design for approximating a desired unitary operator in quantum computing.

Other possible directions include generalizing the results of this paper to the setting of discrete Hamiltonian variational integrators, as introduced in Lall and West [19], and Leok and Zhang [25], or extensions to problems with nonholonomic constraints, as discussed in Cortés and Martínez [10], Fedorov and Zenkov [11], McLachlan and Perlmutter [32], and Kobilarov et al. [18]. Additionally, stochastic variational integrators have been studied in Bou-Rabee and Owhadi [4,5], and it would be natural to consider the synthesis of such methods with Lie group variational integrators.

6.1.4 Parallel Implementation and Computational Efficiency

Perhaps our method's greatest flaw is that it requires the solution of a large number of nonlinear equations at every time-step. This problem is further exasperated by the fact that assembling the Newton matrix at every time-step requires the repeated application of a high-order quadrature rule. While the fact that our method is capable of taking very large time-steps helps to overcome this computational difficulty, it would be interesting to see how much our method could be accelerated by assembling our Newton matrix in parallel.

6.1.5 Multisymplectic Variational Integrators

Multisymplectic geometry, as described in Marsden et al. [29], has become an increasingly popular framework for extending much of the geometric theory from classical Lagrangian mechanics to Lagrangian PDEs. The foundations for a discrete theory have been laid in Lew et al. [26] and Vankerschaver et al. [39], and there have been significant results achieved in geometric techniques for structured problems such as elasticity, fluid mechanics, nonlinear wave equations, and computational electromagnetism. However, there is still significant work to be done in the areas of construction of numerical methods, analysis of discrete geometric structure, and especially error analysis. Galerkin type methods have become a standard in classical numerical PDE methods, popular examples include finite-element, spectral, and pseudospectral methods. The variational Galerkin framework could provide a natural framework for extending these classical methods to structure-preserving geometric methods for PDEs.

Acknowledgements This work was supported in part by NSF Grants CMMI-1029445, DMS-1065972, CMMI-1334759, DMS-1411792, DMS-1345013, and NSF CAREER Award DMS-1010687.

7 Appendix

7.1 Proof of Theorem 3.2

In Sect. 3.1.2, we stated Theorem 3.2 but did not provide a proof. This is because the proof is essentially the same as that for optimal convergence, with slight and obvious modifications. For completeness, we will provide the proof here.

Theorem 7.1 *Given an interval $[0, h]$, and a Lagrangian $L : TG \rightarrow \mathbb{R}$, suppose that $\tilde{g}(t)$ solves the Euler–Lagrange equations on that interval exactly. Furthermore, suppose that the exact solution $\tilde{g}(t)$ falls within the range of the natural chart, that is:*

$$\tilde{g}(t) = L_{g_k} \Phi(\tilde{\eta}(t))$$

for some $\tilde{\eta} \in C^2([0, h], \mathfrak{g})$. For the function space $\mathbb{M}^n([0, h], \mathfrak{g})$ and the quadrature rule \mathcal{G} , define the Galerkin discrete Lagrangian $L_d^G(g_0, g_1) \rightarrow \mathbb{R}$ as

$$\begin{aligned} L_d^G(g_0, g_1, n) &= \underset{\substack{g_n \in \mathbb{GM}^n(g_0 \times [0, h], G) \\ g_n(0) = g_0, g_n(h) = g_1}}{\text{ext}} h \sum_{j=1}^m b_j L(g_n(c_j h), \dot{g}_n(c_j h)) \\ &= h \sum_{h=1}^m b_j L(\tilde{g}_n(c_j h), \dot{\tilde{g}}_n(c_j h)) \end{aligned} \tag{30}$$

where $\tilde{g}_n(t)$ is the extremizing curve in $\mathbb{GM}^n(g_0 \times [0, h], G)$. If:

- (1) there exists an approximation $\hat{\eta} \in \mathbb{M}^n([0, h], \mathfrak{g})$ such that,

$$\begin{aligned} \|\tilde{\eta} - \hat{\eta}, \tilde{\eta} - \hat{\eta}\|^{\frac{1}{2}} &\leq C_A K_A^n \\ \|\dot{\tilde{\eta}} - \dot{\hat{\eta}}, \dot{\tilde{\eta}} - \dot{\hat{\eta}}\|^{\frac{1}{2}} &\leq C_{\mathfrak{A}} K_A^n, \end{aligned}$$

for some constants $C_A \geq 0$ and $C_{\mathfrak{A}} \geq 0, 0 < K_A < 1$ independent of n ,

- (2) the Lagrangian L is Lipschitz in the chosen error norm in both its arguments, that is:

$$|L(g_1, \dot{g}_1) - L(g_2, \dot{g}_2)| \leq L_\alpha (e_g(g_1, g_2) + e_a(\dot{g}_1, \dot{g}_2))$$

- (3) the chart function Φ is well conditioned in $e_g(\cdot, \cdot)$ and $e_a(\cdot, \cdot)$, that is (9) and (10) hold,
- (4) there exists a sequence of quadrature rules $\{\mathcal{G}_n\}_{n=1}^\infty, \mathcal{G}_n(f) = h \sum_{j=1}^{m_n} b_{n_j} f(c_{n_j} h) \approx \int_0^h f(t) dt$, and there exists a constant $0 < K_g < 1$ independent of n such that,

$$\left| \int_0^h L(g_n(t), \dot{g}_n(t)) dt - h \sum_{j=1}^{m_n} b_{n_j} L(g_n(c_{n_j} h), \dot{g}_n(c_{n_j} h)) \right| \leq C_g K_g^n$$

for any $g_n(t) = L_{g_0} \Phi(\xi(t))$ where $\xi \in \mathbb{M}^n([0, h], \mathfrak{g})$,

- (5) the stationary points of the discrete action and the continuous action are minimizers,

then the variational integrator induced by $L_d^G(g_0, g_1, n)$ has error $\mathcal{O}(K_s^n)$ for some constant K_s independent of n , $0 < K_s < 1$.

Proof We begin by rewriting the exact discrete Lagrangian and the Galerkin discrete Lagrangian:

$$\begin{aligned} & \left| L_d^E(g_0, g_1, n) - L_d^G(g_0, g_1, h) \right| \\ &= \left| \int_0^h L(\bar{g}, \dot{\bar{g}}) dt - h \sum_{j=1}^{m_n} b_{n_j} L(\tilde{g}_n(c_{n_j}h), \dot{\tilde{g}}_n(c_{n_j}h)) \right|, \end{aligned}$$

where we have introduced \tilde{g}_n , which is the stationary point of the local Galerkin action (30). We introduce the solution in the approximation space which takes the form $\hat{g}_n(t) = L_{g_k} \Phi(\hat{\eta}(t))$, and compare the action on the exact solution to the action on this solution:

$$\begin{aligned} \left| \int_0^h L(\bar{g}, \dot{\bar{g}}) dt - \int_0^h L(\hat{g}_n, \dot{\hat{g}}_n) dt \right| &= \left| \int_0^h L(\bar{g}, \dot{\bar{g}}) - L(\hat{g}_n, \dot{\hat{g}}_n) dt \right| \\ &\leq \int_0^h \left| L(\bar{g}, \dot{\bar{g}}) - L(\hat{g}_n, \dot{\hat{g}}_n) \right| dt. \end{aligned}$$

Now, we use the Lipschitz assumption to establish the bound

$$\begin{aligned} \int_0^h \left| L(\bar{g}, \dot{\bar{g}}) - L(\hat{g}_n, \dot{\hat{g}}_n) \right| dt &\leq \int_0^h L_\alpha \left(e_g(\bar{g}, \hat{g}_n) + e_a(\dot{\bar{g}}, \dot{\hat{g}}_n) \right) dt \\ &= \int_0^h L_\alpha \left(e_g(L_{g_k} \Phi(\bar{\eta}), L_{g_k} \Phi(\hat{\eta})) \right. \\ &\quad \left. + e_a(D_{\Phi(\bar{\eta})} L_{g_0} D_{\bar{\eta}} \Phi(\dot{\bar{\eta}}), D_{\Phi(\hat{\eta})} L_{g_0} D_{\hat{\eta}} \Phi(\dot{\hat{\eta}})) \right) dt, \end{aligned}$$

and the chart conditioning assumptions to see

$$\begin{aligned} \int_0^h \left| L(\bar{g}, \dot{\bar{g}}) - L(\hat{g}_n, \dot{\hat{g}}_n) \right| dt &\leq \int_0^h L_\alpha \left(C_G \langle \bar{\eta} - \hat{\eta}, \bar{\eta} - \hat{\eta} \rangle^{\frac{1}{2}} + C_g \langle \dot{\bar{\eta}} - \dot{\hat{\eta}}, \dot{\bar{\eta}} - \dot{\hat{\eta}} \rangle^{\frac{1}{2}} \right. \\ &\quad \left. + C_g^G \langle \bar{\eta} - \hat{\eta}, \bar{\eta} - \hat{\eta} \rangle^{\frac{1}{2}} \right) dt \\ &\leq \int_0^h L_\alpha \left(C_G C_A K_A^n + C_g C_{2l} K_A^n + C_g^G C_A K_A^n \right) dt \\ &= L_\alpha \left((C_G + C_g^G) C_A + C_g C_{2l} \right) K_A^n. \end{aligned}$$

This establishes a bound between the action evaluated on the exact discrete Lagrangian and the optimal solution in the approximation space. Considering the Galerkin discrete action,

$$\begin{aligned}
 h \sum_{j=1}^{m_n} b_{n_j} L(\tilde{g}_n, \tilde{g}_n) &\leq h \sum_{j=1}^{m_n} b_{n_j} L(\hat{g}_n, \dot{\hat{g}}_n) \\
 &\leq \int_0^h L(\hat{g}_n, \dot{\hat{g}}_n) dt + C_g K_g^n \\
 &\leq \int_0^h L(\bar{g}, \dot{\bar{g}}) dt + C_g K_g^n + L_\alpha \left((C_G + C_g^G) C_A + C_g C_{\mathfrak{A}} \right) K_A^n
 \end{aligned}
 \tag{31}$$

where we have used the assumption that the Galerkin approximation minimizes the Galerkin discrete action and the assumption on the accuracy of the quadrature. Now, using the fact that $\bar{g}(t)$ minimizes the action and that $\mathbb{G}\mathbb{M}^n(g_0 \times [0, h], G) \subset C^2([0, h], G)$,

$$\begin{aligned}
 h \sum_{j=1}^{m_n} b_{n_j} L(\tilde{g}_n, \dot{\tilde{g}}_n) &\geq \int_0^h L(\tilde{g}_n, \dot{\tilde{g}}_n) dt - C_g K_g^n \\
 &\geq \int_0^h L(\bar{g}, \dot{\bar{g}}) dt - C_g K_g^n.
 \end{aligned}
 \tag{32}$$

Combining inequalities (31) and (32), we see that,

$$\begin{aligned}
 \int_0^h L(\bar{g}, \dot{\bar{g}}) dt - C_g K_g^n &\leq h \sum_{j=1}^{m_n} b_{n_j} L(\tilde{g}_n, \dot{\tilde{g}}_n) \leq \int_0^h L(\bar{g}, \dot{\bar{g}}) dt + C_g K_g^n \\
 &\quad + L_\alpha \left((C_G + C_g^G) C_A + C_g C_{\mathfrak{A}} \right) K_A^n
 \end{aligned}$$

which implies

$$\left| \int_0^h L(\bar{g}, \dot{\bar{g}}) dt - h \sum_{j=1}^{m_n} b_{n_j} L(\tilde{g}_n, \dot{\tilde{g}}_n) \right| \leq \left(C_g + L_\alpha \left((C_G + C_g^G) C_A + C_g C_{\mathfrak{A}} \right) \right) K_s^n
 \tag{33}$$

where $K_s = \max(K_A, K_g)$. The left-hand side of (33) is exactly $|L_d^E(g_0, g_1, h) - L_d^G(g_0, g_1, n)|$, and thus

$$\left| L_d^E(g_0, g_1, h) - L_d^G(g_0, g_1, n) \right| \leq \left(C_g + L_\alpha \left((C_G + C_g^G) C_A + C_g C_{\mathfrak{A}} \right) \right) K_s^n.$$

This states that the Galerkin discrete Lagrangian approximates the exact discrete Lagrangian with error $\mathcal{O}(K_s^n)$, and by Theorem (1.1) this further implies that the Lagrangian update map has error $\mathcal{O}(K_s^n)$. \square

7.2 Proof of bound from Lemma 3.1

In the proof of Lemma 3.1, we stated but did not prove the bound (18)

$$\nabla^2 K(\eta(t), \dot{\eta}(t)) [(\delta\xi, \delta\dot{\xi})] [(\delta\xi, \delta\dot{\xi})] \geq C_{\dot{\xi}} \delta\dot{\xi}(t)^T \delta\dot{\xi}(t) - C_{\xi} \delta\xi(t)^T \delta\xi(t).$$

We provide the proof of this bound below.

Proof Considering K , note that

$$R(\xi(t))^T \dot{R}(\xi(t)) = \Phi(\xi(t))^T \nabla\Phi(\xi(t)) \dot{\xi}(t)$$

and hence as a function of $\dot{\xi}(t)$,

$$K(\dot{\xi}(t)) = \dot{\xi}(t)^T \nabla\Phi(\xi(t))^T \Phi(\xi(t)) J_d \Phi(\xi(t))^T \nabla\Phi(\xi(t)) \dot{\xi}(t).$$

J_d is a diagonal matrix with (J_1, J_2, J_3) on the diagonal, and because $\Phi(\xi(t))$ is an orthogonal matrix, $\Phi(\xi(t)) J_d \Phi(\xi(t))^T$ has the eigenvalues (J_1, J_2, J_3) . Furthermore, $\Phi(\cdot)$ is a diffeomorphism, which implies $\nabla\Phi(\cdot)$ is non-singular, so

$$\begin{aligned} & \dot{\xi}(t)^T \nabla\Phi(\xi(t))^T \Phi(\xi(t)) J_d \Phi(\xi(t))^T \nabla\Phi(\xi(t)) \dot{\xi}(t) \\ & \geq J_{\min} \|\nabla\Phi(\xi(t)) \dot{\xi}(t)\|_2^2 \\ & \geq J_{\min} |\sigma_{\min}(t)| \|\dot{\xi}(t)\|_2^2 \end{aligned}$$

where $J_{\min} = \min\{J_1, J_2, J_3\}$ and $\sigma_{\min}(t)$ is the value of $\nabla\Phi(\dot{\xi}(t))$ with smallest magnitude. Since $|\sigma_{\min}(t)|$ is a continuous function of t and $|\sigma_{\min}(t)| > 0$ for all t over the compact interval $[0, h]$, there exists a constant $C_{\sigma} > 0$ such that $|\sigma_{\min}(t)| > C_{\sigma}$ for all $t \in [0, h]$. Finally, we note

$$\begin{aligned} & \frac{\partial^2 K}{\partial \dot{\xi}^2}(\eta(t), \dot{\eta}(t)) [\delta\dot{\xi}_a] [\delta\dot{\xi}_b] \\ & = 2\delta\dot{\xi}_a^T \nabla\Phi(\eta(t))^T \Phi(\eta(t)) J_d \Phi(\eta(t))^T \nabla\Phi(\eta(t)) \delta\dot{\xi}_b, \end{aligned}$$

and hence

$$\frac{\partial^2 K}{\partial \dot{\xi}^2}(\eta(t), \dot{\eta}(t)) [\delta\dot{\xi}] [\delta\dot{\xi}] \geq 2J_{\min} C_{\sigma} \delta\dot{\xi}^T \delta\dot{\xi}. \tag{34}$$

Now, considering the full term $\nabla^2 K (\eta (t) , \dot{\eta} (t)) [(\delta\xi , \delta\dot{\xi})] [(\delta\xi , \delta\dot{\xi})]$, we see that:

$$\begin{aligned} \nabla^2 K (\eta (t) , \dot{\eta} (t)) [(\delta\xi , \delta\dot{\xi})] [(\delta\xi , \delta\dot{\xi})] &= \frac{\partial^2 K}{\partial \xi^2} (\eta (t) , \dot{\eta} (t)) [\delta\xi] [\delta\xi] \\ &\quad + 2 \frac{\partial^2 K}{\partial \xi \partial \dot{\xi}} (\eta (t) , \dot{\eta} (t)) [\delta\xi] [\delta\dot{\xi}] \\ &\quad + \frac{\partial^2 K}{\partial \dot{\xi}^2} (\eta (t) , \dot{\eta} (t)) [\delta\dot{\xi}] [\delta\dot{\xi}], \end{aligned} \tag{35}$$

where we have made use of the symmetry of mixed second derivatives. K is smooth in all of its components, and hence there exists $C_m > 0, C_d > 0$ such that

$$\frac{\partial^2 K}{\partial \xi \partial \dot{\xi}} (\eta (t) , \dot{\eta} (t)) [\delta\xi] [\delta\dot{\xi}] \geq -C_m \delta\xi^T \delta\dot{\xi} \tag{36}$$

$$\frac{\partial^2 K}{\partial \xi^2} (\eta (t) , \dot{\eta} (t)) [\delta\xi] [\delta\xi] \geq -C_d \delta\xi^T \delta\xi. \tag{37}$$

Defining $C_p = 2J_{\min}C_\sigma$, inserting (34), (36), and (37) into (35) gives

$$\begin{aligned} &\nabla^2 K (\eta (t) , \dot{\eta} (t)) [(\delta\xi , \delta\dot{\xi})] [(\delta\xi , \delta\dot{\xi})] \\ &\geq C_p \delta\dot{\xi} (t)^T \delta\dot{\xi} (t) - C_m \delta\dot{\xi} (t)^T \delta\xi (t) - C_d \delta\xi (t)^T \delta\xi (t) \\ &= \frac{C_p}{2} \delta\dot{\xi} (t)^T \delta\dot{\xi} (t) + \frac{C_p}{2} \delta\dot{\xi} (t)^T \delta\dot{\xi} (t) - C_m \delta\dot{\xi} (t)^T \delta\xi (t) \\ &\quad - C_d \delta\xi (t)^T \delta\xi (t). \end{aligned}$$

Completing the square, we see that

$$\begin{aligned} &\frac{C_p}{2} \delta\dot{\xi} (t)^T \delta\dot{\xi} (t) + \frac{C_p}{2} \delta\dot{\xi} (t)^T \delta\dot{\xi} (t) - C_m \delta\dot{\xi} (t)^T \delta\xi (t) - C_d \delta\xi (t)^T \delta\xi (t) \\ &= \frac{C_p}{2} \delta\dot{\xi} (t)^T \delta\dot{\xi} (t) + \left(\frac{\sqrt{C_p}}{\sqrt{2}} \delta\dot{\xi} (t) - \frac{\sqrt{2}C_m}{2\sqrt{C_p}} \delta\xi (t) \right)^T \\ &\quad \left(\frac{\sqrt{C_p}}{\sqrt{2}} \delta\dot{\xi} (t) - \frac{\sqrt{2}C_m}{2\sqrt{C_p}} \delta\xi (t) \right) \\ &\quad - \left(C_d + \frac{C_m^2}{2C_p} \right) \delta\xi (t)^T \delta\xi (t) \\ &= \frac{C_p}{2} \|\delta\dot{\xi} (t)\|_2^2 + \left\| \frac{\sqrt{C_p}}{\sqrt{2}} \delta\dot{\xi} (t) - \frac{\sqrt{2}C_m}{2\sqrt{C_p}} \delta\xi (t) \right\|_2^2 - \left(C_d + \frac{C_m^2}{2C_p} \right) \|\delta\xi (t)\|_2^2. \end{aligned}$$

Making use of the trivial bound that for any $a, b \in \mathbb{R}^3$, $\|a - b\|_2^2 \geq 0$, we see

$$\begin{aligned} & \frac{C_p}{2} \|\delta\dot{\xi}(t)\|_2^2 + \left\| \frac{\sqrt{C_p}}{\sqrt{2}} \delta\dot{\xi}(t) - \frac{\sqrt{2}C_m}{2\sqrt{C_p}} \delta\xi(t) \right\|_2^2 - \left(C_d + \frac{C_m^2}{2C_p} \right) \|\delta\xi(t)\|_2^2 \\ & \geq \frac{C_p}{2} \|\delta\dot{\xi}(t)\|_2^2 - \left(C_d + \frac{C_m^2}{2C_p} \right) \|\delta\xi(t)\|_2^2 \\ & = C_{\dot{\xi}} \delta\dot{\xi}(t)^T \delta\dot{\xi}(t) - C_{\xi} \delta\xi(t)^T \delta\xi(t) \end{aligned}$$

for constants $C_{\dot{\xi}} > 0$, $C_{\xi} > 0$, where

$$\begin{aligned} C_{\dot{\xi}} &= \frac{C_p}{2} \\ C_{\xi} &= C_d + \frac{C_m^2}{2C_p}. \end{aligned}$$

This bound allows us to conclude

$$\nabla^2 K(\eta(t), \dot{\eta}(t)) [(\delta\xi, \delta\dot{\xi})] [(\delta\xi, \delta\dot{\xi})] \geq C_{\dot{\xi}} \dot{\xi}(t)^T \dot{\xi}(t) - C_{\xi} \xi(t)^T \xi(t).$$

□

7.3 Proof of Lemma 3.2

In Sect. 3.3, we stated Lemma 3.2 but did not prove it. We provide the proof below.

Lemma 7.1 *For Lagrangians on $SO(3)$ of the form*

$$L(R, \dot{R}) = \text{tr}(\dot{R}^T R J_d R^T \dot{R}) - V(R),$$

there exists a $C > 0$ such that for $h < C$, the second Frechet derivative of $\mathfrak{S}_{\mathfrak{g}}(\cdot, \cdot)$ at $(\bar{\eta}(t), \dot{\bar{\eta}}(t))$ is coercive on the interval $[0, h]$.

Proof First, we note that for this Lagrangian

$$\begin{aligned} & D^2 \mathfrak{S}_{\mathfrak{g}}(\bar{\eta}(t), \dot{\bar{\eta}}(t)) [(\delta\xi(t), \delta\dot{\xi}(t))] [(\delta\xi(t), \delta\dot{\xi}(t))] \\ & = \int_0^h \nabla^2 L \left(L_{g_k} \Phi(\bar{\eta}(t)), \frac{d}{dt} L_{g_k} \Phi(\bar{\eta}(t)) \right) [(\delta\xi(t), \delta\dot{\xi}(t))] [(\delta\xi(t), \delta\dot{\xi}(t))] dt \end{aligned}$$

From the proof of Lemma 3.1, we know that

$$\begin{aligned} & \nabla^2 L \left(L_{g_k} \Phi(\bar{\eta}(t)), \frac{d}{dt} L_{g_k} \Phi(\bar{\eta}(t)) \right) [(\delta\xi(t), \delta\dot{\xi}(t))] [(\delta\xi(t), \delta\dot{\xi}(t))] \\ & \geq C_{\dot{\xi}} \delta\dot{\xi}(t)^T \delta\dot{\xi}(t) - (C_{\xi} + C_V) \delta\xi(t)^T \delta\xi(t) \\ & = \frac{C_{\dot{\xi}}}{2} \delta\dot{\xi}(t)^T \delta\dot{\xi}(t) + \frac{C_{\dot{\xi}}}{2} \delta\dot{\xi}(t)^T \delta\dot{\xi}(t) - (C_{\xi} + C_V) \delta\xi(t)^T \delta\xi(t), \end{aligned}$$

and hence

$$\begin{aligned}
 & D^2\mathfrak{S}_{\mathbf{g}}(\bar{\eta}(t), \dot{\bar{\eta}}(t)) [(\delta\xi(t), \delta\dot{\xi}(t))] [(\delta\xi(t), \delta\dot{\xi}(t))] \\
 & \geq \int_0^h \frac{C_{\dot{\xi}}}{2} \delta\dot{\xi}(t)^T \delta\dot{\xi}(t) dt + \int_0^h \frac{C_{\xi}}{2} \delta\xi(t)^T \delta\xi(t) - (C_{\xi} + C_V) \delta\xi(t)^T \delta\xi(t) dt.
 \end{aligned}
 \tag{38}$$

Applying Poincaré’s inequality, we see that

$$\begin{aligned}
 & \int_0^h \frac{C_{\dot{\xi}}}{2} \delta\dot{\xi}(t)^T \delta\dot{\xi}(t) dt - \int_0^h (C_{\xi} + C_V) \delta\xi(t)^T \delta\xi(t) dt \\
 & \geq \frac{C_{\dot{\xi}}\pi^2}{2h^2} \int_0^h \delta\xi(t)^T \delta\xi(t) dt - (C_{\xi} + C_V) \int_0^h \delta\xi(t)^T \delta\xi(t) dt \\
 & = \left(\frac{C_{\dot{\xi}}\pi^2}{2h^2} - (C_{\xi} + C_V) \right) \int_0^h \delta\xi(t)^T \delta\xi(t) dt.
 \end{aligned}
 \tag{39}$$

Replacing the last two terms in (38) with (39), we see

$$\begin{aligned}
 & D^2\mathfrak{S}_{\mathbf{g}}((\bar{\eta}, \dot{\bar{\eta}})) [(\delta\xi(t), \delta\dot{\xi}(t))] [(\delta\xi(t), \delta\dot{\xi}(t))] \\
 & \geq \frac{C_{\dot{\xi}}}{2} \int_0^h \delta\dot{\xi}(t)^T \delta\dot{\xi}(t) dt + \left(\frac{C_{\dot{\xi}}\pi^2}{2h^2} - (C_{\xi} + C_V) \right) \int_0^h \delta\xi(t)^T \delta\xi(t) dt \\
 & = \frac{C_{\dot{\xi}}}{2} \|\delta\dot{\xi}(t)\|_{L^2([0,h])}^2 + \left(\frac{C_{\dot{\xi}}\pi^2}{2h^2} - (C_{\xi} + C_V) \right) \|\delta\xi(t)\|_{L^2([0,h])}^2.
 \end{aligned}$$

We now apply Hölder’s inequality

$$\|fg\|_{L^1([0,h])} \leq \|f\|_{L^2([0,h])} \|g\|_{L^2([0,h])}$$

to derive the bounds

$$\begin{aligned}
 \|\delta\dot{\xi}(t)\|_{L^1([0,h])} & \leq \sqrt{h} \|\delta\dot{\xi}(t)\|_{L^2([0,h])} \\
 \|\delta\xi(t)\|_{L^1([0,h])} & \leq \sqrt{h} \|\delta\xi(t)\|_{L^2([0,h])},
 \end{aligned}$$

and hence,

$$\begin{aligned}
 & D^2\mathfrak{S}_{\mathbf{g}}((\bar{\eta}, \dot{\bar{\eta}})) [(\delta\xi(t), \delta\dot{\xi}(t))] [(\delta\xi(t), \delta\dot{\xi}(t))] \\
 & \geq \frac{C_{\dot{\xi}}}{2h} \|\delta\dot{\xi}(t)\|_{L^1([0,h])}^2 + \frac{1}{h} \left(\frac{C_{\dot{\xi}}\pi^2}{2h^2} - (C_{\xi} + C_V) \right) \|\delta\xi(t)\|_{L^1([0,h])}^2 \\
 & \geq \min \left(\frac{C_{\dot{\xi}}}{2h}, \frac{1}{h} \left(\frac{C_{\dot{\xi}}\pi^2}{2h^2} - (C_{\xi} + C_V) \right) \right) \left(\|\delta\xi(t)\|_{L^1([0,h])}^2 + \|\delta\dot{\xi}(t)\|_{L^1([0,h])}^2 \right)
 \end{aligned}$$

$$\begin{aligned} &\geq \min\left(\frac{C_\xi}{2h}, \frac{1}{h}\left(\frac{C_\xi\pi^2}{2h^2} - (C_\xi + C_V)\right)\right)\left(\frac{1}{2}\right) \\ &\quad \left(\|\delta\xi(t)\|_{L^1([0,h])} + \|\delta\dot{\xi}(t)\|_{L^1([0,h])}\right)^2 \\ &\geq \min\left(\frac{C_\xi}{4h}, \frac{1}{2h}\left(\frac{C_\xi\pi^2}{2h^2} - (C_\xi + C_V)\right)\right)\|\delta\xi(t)\|_{W^{1,1}([0,h])}^2 \end{aligned}$$

which establishes the required coercivity result so long as $0 < h < \sqrt{\frac{C_\xi\pi^2}{2(C_\xi+C_V)}}$. \square

7.4 Proof of Lemma 4.1

Finally, in Sect. 4.2.1, we establish Lemma 4.1, which shows that the natural chart based on the Cayley transform is well conditioned. We provide the proof of this below.

Lemma 7.2 *For $\eta, v \in \mathfrak{so}(3)$, so long as*

$$2\|\eta\|_2 + \|v\|_2 < 1, \tag{40}$$

the natural chart constructed by the Cayley transform locally satisfies chart conditioning assumption, that is:

$$\begin{aligned} \|\Phi(\eta) - \Phi(v)\|_2 &\leq C_G \langle \eta - v, \eta - v \rangle^{\frac{1}{2}} \\ \|D_\eta\Phi(\dot{\eta}) - D_v\Phi(\dot{v})\|_2 &\leq C_g \langle \eta - v, \eta - v \rangle^{\frac{1}{2}} + C_g^G \langle \dot{\eta} - \dot{v}, \dot{\eta} - \dot{v} \rangle^{\frac{1}{2}}. \end{aligned}$$

If $\|\eta - v\|_2 < \epsilon$, assumption (26) can be relaxed to

$$\|\eta\|_2 + \epsilon < 1.$$

Proof Throughout the proof of this lemma, we will make extensive use of two inequalities. The first is the bound:

$$\|(I + E)^{-1}\|_p \leq (1 - \|E\|_p)^{-1}, \tag{41}$$

if $\|E\|_p < 1$, and the second is the bound:

$$\|(A + E)^{-1} - A^{-1}\|_p \leq \|E\|_p \|A^{-1}\|_p^2 \left(1 - \|A^{-1}E\|_p\right)^{-1} \tag{42}$$

which generalizes (41). We begin with

$$\begin{aligned} \|\Phi(\eta) - \Phi(v)\|_2 &= \|(I - \eta)(I + \eta)^{-1} - (I - v)(I + v)^{-1}\|_2 \\ &= \|(I - \eta)(I + \eta)^{-1} - (I - \eta)(I + v)^{-1} \end{aligned}$$

$$\begin{aligned}
 & + (I - \eta) (I + \nu)^{-1} - (I - \nu) (I + \nu)^{-1} \Big\|_2 \\
 = & \left\| (I - \eta) \left[(I + \eta)^{-1} - (I + \nu)^{-1} \right] \right. \\
 & \left. + [(I - \eta) - (I - \nu)] (I + \nu)^{-1} \right\|_2 \\
 = & \left\| (I - \eta) \left[(I + \eta)^{-1} - (I + \nu)^{-1} \right] + [\nu - \eta] (I + \nu)^{-1} \right\|_2 \\
 \leq & \left\| (I - \eta) \left[(I + \eta)^{-1} - (I + \nu)^{-1} \right] \right\|_2 + \left\| [\nu - \eta] (I + \nu)^{-1} \right\|_2.
 \end{aligned} \tag{43}$$

Considering the term $[\nu - \eta] (I + \nu)^{-1}$, we make use of (41) to see

$$\begin{aligned}
 \left\| [\nu - \eta] (I + \nu)^{-1} \right\|_2 & \leq \|\nu - \eta\|_2 \left\| (I + \nu)^{-1} \right\|_2 \\
 & \leq (1 - \|\nu\|_2)^{-1} \|\eta - \nu\|_2.
 \end{aligned} \tag{44}$$

Next, considering the term $\left\| (I - \eta) \left[(I + \eta)^{-1} - (I + \nu)^{-1} \right] \right\|_2$,

$$\begin{aligned}
 \left\| (I - \eta) \left[(I + \eta)^{-1} - (I + \nu)^{-1} \right] \right\|_2 & \leq \|I - \eta\|_2 \left\| (I + \eta)^{-1} - (I + \nu)^{-1} \right\|_2 \\
 & = \|I - \eta\|_2 \left\| (I + \nu + (\eta - \nu))^{-1} - (I + \nu)^{-1} \right\|_2.
 \end{aligned} \tag{45}$$

Applying (42), with $E = \eta - \nu$ and $A = I + \nu$,

$$\begin{aligned}
 & \left\| (I + \nu + (\eta - \nu))^{-1} - (I + \nu)^{-1} \right\|_2 \\
 & \leq \|\eta - \nu\|_2 \left\| (I + \nu)^{-1} \right\|_2^2 \left(1 - \left\| (I + \nu)^{-1} (\eta - \nu) \right\|_2 \right)^{-1}.
 \end{aligned} \tag{46}$$

But

$$\begin{aligned}
 1 - \left\| (I + \nu)^{-1} (\eta - \nu) \right\|_2 & \geq 1 - \left\| (I + \nu)^{-1} \right\|_2 \|\eta - \nu\|_2 \\
 & \geq 1 - (1 - \|\nu\|_2)^{-1} \|\eta - \nu\|_2
 \end{aligned}$$

which implies

$$\left(1 - \left\| (I + \nu)^{-1} (\eta - \nu) \right\|_2 \right)^{-1} \leq \left(1 - (1 - \|\nu\|_2)^{-1} \|\eta - \nu\|_2 \right)^{-1}$$

and

$$\left\| (I + \nu)^{-1} \right\|_2^2 \leq (1 - \|\nu\|_2)^{-2},$$

so

$$\begin{aligned} & \left\| (I + v)^{-1} \right\|_2^2 \left(1 - \left\| (I + v)^{-1} (\eta - v) \right\|_2 \right)^{-1} \\ & \leq (1 - \|v\|_2)^{-2} \left(1 - (1 - \|v\|_2)^{-1} \|(\eta - v)\|_2 \right)^{-1} \\ & \leq (1 - \|v\|_2)^{-1} \left((1 - \|v\|_2) - \|\eta - v\|_2 \right)^{-1} \\ & = (1 - \|v\|_2)^{-1} (1 - \|v\|_2 - \|\eta - v\|_2)^{-1}. \end{aligned} \tag{47}$$

The triangle inequality gives

$$\|\eta - v\|_2 \leq \|\eta\|_2 + \|v\|_2$$

and thus

$$\begin{aligned} 1 - \|\eta\|_2 - \|\eta - v\|_2 & \geq 1 - 2\|\eta\|_2 - \|v\|_2 \\ (1 - \|\eta\|_2 - \|\eta - v\|_2)^{-1} & \leq (1 - 2\|\eta\|_2 - \|v\|_2)^{-1}. \end{aligned} \tag{48}$$

So applying (48) to (47) gives,

$$\left\| (I + v)^{-1} \right\|_2^2 \left(1 - \left\| (I + v)^{-1} (\eta - v) \right\|_2 \right)^{-1} \leq (1 - \|v\|_2)^{-1} (1 - 2\|\eta\|_2 - \|v\|_2)^{-1}, \tag{49}$$

then applying (49) to (46) gives,

$$\left\| (I + v + (\eta - v))^{-1} - (I + v)^{-1} \right\|_2 \leq \|\eta - v\|_2 (1 - \|v\|_2)^{-1} (1 - 2\|\eta\|_2 - \|v\|_2)^{-1}, \tag{50}$$

and finally applying (50) to (45) yields

$$\begin{aligned} & \left\| (I - \eta) \left[(I + \eta)^{-1} - (I + v)^{-1} \right] \right\|_2 \\ & \leq \|I - \eta\|_2 (1 - \|v\|_2)^{-1} (1 - 2\|\eta\|_2 - \|v\|_2)^{-1} \|\eta - v\|_2 \\ & \leq (1 - \|\eta\|_2)^{-1} (1 - \|v\|_2)^{-1} (1 - 2\|\eta\|_2 - \|v\|_2)^{-1} \|\eta - v\|_2. \end{aligned} \tag{51}$$

Substituting (44) and (51) into (43), we see

$$\begin{aligned} & \|\Phi(\eta) - \Phi(v)\|_2 \\ & \leq \left[(1 - \|v\|_2)^{-1} + (1 - \|\eta\|_2)^{-1} (1 - \|v\|_2)^{-1} (1 - 2\|\eta\|_2 - \|v\|_2)^{-1} \right] \|\eta - v\|_2. \end{aligned}$$

Hence, so as long as $2\|\eta\| + \|v\| < C_{con} < 1$

$$\|\Phi(\eta) - \Phi(v)\|_2 \leq C_G \|\eta - v\|_2$$

where

$$C_G = \left[(1 - \|v\|_2)^{-1} + (1 - \|\eta\|_2)^{-1} (1 - \|v\|_2)^{-1} (1 - 2\|\eta\|_2 - \|v\|_2)^{-1} \right].$$

If we make the stronger assumption that $\|\eta - v\|_2 < \epsilon$, we can weaken the assumption to simply $\|\eta\|_2 + \epsilon < C_{con} < 1$ and $\|v\|_2 + \epsilon < C_{con} < 1$. As we expect the error between the two curves in the Lie algebra to be orders of magnitude smaller than the magnitude of the Lie algebra elements, this is a reasonable assumption to make.

Next, to examine $\|D_\eta \Phi(\dot{\eta}) - D_v \Phi(\dot{v})\|_2$, we consider the definition

$$D_X \Phi(Y) = -Y(I + X)^{-1} - (I - X)(I + X)^{-1}Y(I + X)^{-1}.$$

Using this definition,

$$\begin{aligned} & \|D_\eta \Phi(\dot{\eta}) - D_v \Phi(\dot{v})\|_2 \\ &= \left\| -\dot{\eta}(I + \eta)^{-1} - (I - \eta)(I + \eta)^{-1}\dot{\eta}(I + \eta)^{-1} \right. \\ & \quad \left. + \dot{v}(I + v)^{-1} + (I - v)(I + v)^{-1}\dot{v}(I + v)^{-1} \right\|_2 \\ & \leq \left\| \dot{v}(I + v)^{-1} - \dot{\eta}(I + \eta)^{-1} \right\|_2 \\ & \quad + \left\| (I - v)(I + v)^{-1}\dot{v}(I + v)^{-1} - (I - \eta)(I + \eta)^{-1}\dot{\eta}(I + \eta)^{-1} \right\|_2. \end{aligned}$$

Considering

$$\begin{aligned} & \left\| \dot{v}(I + v)^{-1} - \dot{\eta}(I + \eta)^{-1} \right\|_2 \\ &= \left\| \dot{v}(I + v)^{-1} - \dot{\eta}(I + v)^{-1} + \dot{\eta}(I + v)^{-1} - \dot{\eta}(I + \eta)^{-1} \right\|_2 \\ &= \left\| (\dot{v} - \dot{\eta})(I + v)^{-1} + \dot{\eta} \left[(I + v)^{-1} - (I + \eta)^{-1} \right] \right\|_2 \\ & \leq \left\| (I + v)^{-1} \right\|_2 \|\dot{\eta} - \dot{v}\|_2 + \|\dot{\eta}\|_2 \left\| (I + v)^{-1} - (I + \eta)^{-1} \right\|_2 \\ & \leq (1 - \|v\|_2)^{-1} \|\dot{\eta} - \dot{v}\|_2 + \|\dot{\eta}\|_2 \left((1 - \|v\|_2)(1 - \|v\|_2 - \|v - \eta\|_2) \right)^{-1} \|\eta - v\|_2, \end{aligned}$$

where we have made use of (50) to bound $\|(I + v)^{-1} - (I + \eta)^{-1}\|_2$. Now, considering the second term, we first note,

$$\begin{aligned} & \left\| (I - v)(I + v)^{-1}\dot{v}(I + v)^{-1} - (I - \eta)(I + \eta)^{-1}\dot{\eta}(I + \eta)^{-1} \right\|_2 \\ &= \left\| \Phi(v)\dot{v}(I + v)^{-1} - \Phi(\eta)\dot{\eta}(I + \eta)^{-1} \right\|_2. \end{aligned}$$

Using this, we see

$$\begin{aligned} & \left\| \Phi(v) \dot{v} (I + v)^{-1} - \Phi(\eta) \dot{\eta} (I + \eta)^{-1} \right\|_2 \\ &= \left\| \Phi(v) \dot{v} (I + v)^{-1} - \Phi(v) \dot{v} (I + \eta)^{-1} \right. \\ &\quad \left. + \Phi(v) \dot{v} (I + \eta)^{-1} - \Phi(\eta) \dot{\eta} (I + \eta)^{-1} \right\|_2 \\ &\leq \left\| \Phi(v) \dot{v} (I + v)^{-1} - \Phi(v) \dot{v} (I + \eta)^{-1} \right\|_2 \\ &\quad + \left\| \Phi(v) \dot{v} (I + \eta)^{-1} - \Phi(\eta) \dot{\eta} (I + \eta)^{-1} \right\|_2. \end{aligned} \tag{52}$$

For the first term in (52),

$$\begin{aligned} & \left\| \Phi(v) \dot{v} (I + v)^{-1} - \Phi(v) \dot{v} (I + \eta)^{-1} \right\|_2 \\ &= \left\| \Phi(v) \dot{v} \left[(I + v)^{-1} - (I + \eta)^{-1} \right] \right\|_2 \\ &\leq \|\Phi(v)\|_2 \|\dot{v}\|_2 \left\| (I + v)^{-1} - (I + \eta)^{-1} \right\|_2 \\ &\leq \|\dot{v}\|_2 \left((1 - \|v\|_2) (1 - \|v\|_2 - \|v - \eta\|_2) \right)^{-1} \|\eta - v\|_2, \end{aligned} \tag{53}$$

where we once again have made use of (50) to bound $\|(I + v)^{-1} - (I + \eta)^{-1}\|_2$ and the fact that $\Phi(v)$ is orthogonal to set $\|\Phi(v)\|_2 = 1$. Now, considering the second term in (52),

$$\begin{aligned} \left\| \Phi(v) \dot{v} (I + \eta)^{-1} - \Phi(\eta) \dot{\eta} (I + \eta)^{-1} \right\|_2 &= \left\| (\Phi(v) \dot{v} - \Phi(\eta) \dot{\eta}) (I + \eta)^{-1} \right\|_2 \\ &\leq \|\Phi(v) \dot{v} - \Phi(\eta) \dot{\eta}\|_2 \left\| (I + \eta)^{-1} \right\|_2 \end{aligned} \tag{54}$$

and additionally,

$$\begin{aligned} \|\Phi(v) \dot{v} - \Phi(\eta) \dot{\eta}\|_2 &= \|\Phi(v) \dot{v} - \Phi(\eta) \dot{v} + \Phi(\eta) \dot{v} - \Phi(\eta) \dot{\eta}\|_2 \\ &\leq \|\Phi(v) - \Phi(\eta)\|_2 \|\dot{v}\|_2 + \|\Phi(\eta)\|_2 \|\dot{v} - \dot{\eta}\|_2 \\ &\leq C_G \|\dot{v}\|_2 \|\eta - v\|_2 + \|\dot{\eta} - \dot{v}\|_2. \end{aligned} \tag{55}$$

Combining (53), (54), (55) in (52) yields

$$\left\| D_\eta \Phi(\dot{\eta}) - D_v \Phi(\dot{v}) \right\|_2 \leq C_g \|\eta - v\|_2 + C_g^G \|\dot{\eta} - \dot{v}\|_2$$

with constants

$$\begin{aligned} C_g &= (1 - \|v\|_2 - \|v - \eta\|_2)^{-1} \\ &\quad \left(\|\dot{\eta}\|_2 (1 - \|\eta\|_2)^{-1} + \|\dot{v}\|_2 (1 - \|v\|_2)^{-1} \right) + C_G \|\dot{v}\|_2 \\ C_g^G &= 1 + (1 - \|v\|_2)^{-1}. \end{aligned}$$

To complete the proof of the lemma, we need to establish a bound on the matrix two-norm from the metric on the Lie algebra. For arbitrary algebra element ξ , standard vector and matrix norm equivalences yield

$$\|\hat{\xi}\|_2 \leq \sqrt{3} \|\hat{\xi}\|_1 \leq \sqrt{3} \|\xi\|_1 \leq 3 \|\xi\|_2 = 3 \left\langle \hat{\xi}, \hat{\xi} \right\rangle^{\frac{1}{2}}$$

which completes the proof. \square

References

1. A. I. Bobenko and Y. B. Suris. Discrete time Lagrangian mechanics on Lie groups, with an application to the Lagrange top. *Comm. Math. Phys.*, 204(1):147–188, 1999.
2. G. Bogfjellmo and H. Marthinsen. High-Order Symplectic Partitioned Lie Group Methods. *Found. Comput. Math.*, 2015. doi:10.1007/s10208-015-9257-9.
3. N. Bou-Rabee and J. E. Marsden. Hamilton-Pontryagin integrators on Lie groups. I. Introduction and structure-preserving properties. *Found. Comput. Math.*, 9(2):197–219, 2009.
4. N. Bou-Rabee and H. Owhadi. Stochastic variational integrators. *IMA J. Numer. Anal.*, 29(2):421–443, 2009.
5. N. Bou-Rabee and H. Owhadi. Long-run accuracy of variational integrators in the stochastic context. *SIAM J. Numer. Anal.*, 48(1):278–297, 2010.
6. J. P. Boyd. *Chebyshev and Fourier spectral methods*. Dover Publications Inc., Mineola, NY, second edition, 2001.
7. C. L. Burnett, D. D. Holm, and D. M. Meier. Inexact trajectory planning and inverse problems in the Hamilton-Pontryagin framework. *Proc. R. Soc. Lond. Ser. A Math. Phys. Eng. Sci.*, 469(2160):20130249, 24, 2013.
8. E. Celledoni and B. Owren. Lie group methods for rigid body dynamics and time integration on manifolds. *Comput. Methods Appl. Mech. Engrg.*, 192(3-4):421–438, 2003.
9. P. J. Channell and J. C. Scovel. Integrators for Lie-Poisson dynamical systems. *Phys. D*, 50(1):80–88, 1991.
10. J. Cortés and S. Martínez. Non-holonomic integrators. *Nonlinearity*, 14(5):1365–1392, 2001.
11. Y. N. Fedorov and D. V. Zenkov. Discrete nonholonomic LL systems on Lie groups. *Nonlinearity*, 18(5):2211–2241, 2005.
12. E. Hairer, C. Lubich, and G. Wanner. *Geometric numerical integration*, volume 31 of *Springer Series in Computational Mathematics*. Springer-Verlag, Berlin, second edition, 2006.
13. J. Hall and M. Leok. Spectral Variational Integrators. *Numer. Math.*, 130(4):681–740, 2015.
14. A. Iserles, H. Z. Munthe-Kaas, S. P. Nørsett, and A. Zanna. Lie-group methods. *Acta Numer.*, 9:215–365, 2000.
15. S. M. Jalnapurkar, M. Leok, J. E. Marsden, and M. West. Discrete Routh reduction. *J. Phys. A*, 39(19):5521–5544, 2006.
16. L. O. Jay. Symplectic partitioned Runge-Kutta methods for constrained Hamiltonian systems. *SIAM J. Numer. Anal.*, 33(1):368–387, 1996.
17. L. O. Jay. Structure preservation for constrained dynamics with super partitioned additive Runge-Kutta methods. *SIAM J. Sci. Comput.*, 20(2):416–446, 1998.
18. M. Kobilarov, J. E. Marsden, and G. S. Sukhatme. Geometric discretization of nonholonomic systems with symmetries. *Discrete Contin. Dyn. Syst. Ser. S*, 3(1): 61–84, 2010. ISSN 1937-1632.
19. S. Lall and M. West. Discrete variational Hamiltonian mechanics. *J. Phys. A*, 39(19):5509–5519, 2006.
20. T. Lee, N. H. McClamroch, and M. Leok. A Lie group variational integrator for the attitude dynamics of a rigid body with applications to the 3D pendulum. *Proc. IEEE Conf. on Control Applications*, pages 962–967, 2005. doi:10.1109/CCA.2005.1507254.
21. T. Lee, M. Leok, and N. H. McClamroch. Lie group variational integrators for the full body problem. *Comput. Methods Appl. Mech. Engrg.*, 196(29-30):2907–2924, 2007.
22. T. Lee, M. Leok, and N. H. McClamroch. Lagrangian mechanics and variational integrators on two-spheres. *Internat. J. Numer. Methods Engrg.*, 79(9): 1147–1174, 2009.

23. M. Leok. *Foundations of Computational Geometric Mechanics*. PhD thesis, California Institute of Technology, 2004. URL <http://resolver.caltech.edu/CaltechETD:etd-03022004-000251>.
24. M. Leok and T. Shingel. General techniques for constructing variational integrators. *Front. Math. China*, 7(2):273–303, 2012.
25. M. Leok and J. Zhang. Discrete Hamiltonian variational integrators. *IMA J. Numer. Anal.*, 31(4):1497–1532, 2011.
26. A. Lew, J. E. Marsden, M. Ortiz, and M. West. Asynchronous variational integrators. *Arch. Ration. Mech. Anal.*, 167(2):85–146, 2003.
27. J. E. Marsden and T. S. Ratiu. *Introduction to Mechanics and Symmetry: A Basic Exposition of Classical Mechanical Systems*, volume 17 of *Texts in Applied Mathematics*. Springer-Verlag, New York, second edition, 1999.
28. J. E. Marsden and M. West. Discrete mechanics and variational integrators. *Acta Numer.*, 10:357–514, 2001.
29. J. E. Marsden, G. W. Patrick, and S. Shkoller. Multisymplectic geometry, variational integrators, and nonlinear PDEs. *Comm. Math. Phys.*, 199(2):351–395, 1998.
30. J. E. Marsden, S. Pekarsky, and S. Shkoller. Discrete Euler-Poincaré and Lie-Poisson equations. *Nonlinearity*, 12(6):1647, 1999.
31. J. E. Marsden, S. Pekarsky, and S. Shkoller. Symmetry reduction of discrete Lagrangian mechanics on Lie groups. *J. Geom. Phys.*, 36(1-2):140–151, 2000.
32. R. McLachlan and M. Perlmutter. Integrators for nonholonomic mechanical systems. *J. Nonlinear Sci.*, 16(4):283–328, 2006.
33. R. I. McLachlan and C. Scovel. Equivariant constrained symplectic integration. *J. Nonlinear Sci.*, 5(3):233–256, 1995.
34. R. I. McLachlan, K. Modin, and O. Verdier. Collective Lie-Poisson integrators on \mathbb{R}^3 . *IMA J. Numer. Anal.*, 35(2):546–560, 2015.
35. J. Moser and A.P. Veselov. Discrete versions of some classical integrable systems and factorization of matrix polynomials. *Comm. Math. Phys.*, 139(2):217–243, 1991.
36. T. Ohsawa, A.M. Bloch, and M. Leok. Discrete Hamilton–Jacobi theory. *SIAM J. Control Optim.*, 49(4):1829–1856, 2011.
37. G. W. Patrick and C. Cuell. Error analysis of variational integrators of unconstrained Lagrangian systems. *Numer. Math.*, 113(2):243–264, 2009.
38. L. N. Trefethen. *Spectral methods in MATLAB*, volume 10 of *Software, Environments, and Tools*. Society for Industrial and Applied Mathematics (SIAM), Philadelphia, PA, 2000.
39. J. Vankerschaver, C. Liao, and M. Leok. Generating functionals and Lagrangian partial differential equations. *J. Math. Phys.*, 54(8):082901, 22, 2013.
40. G. Zhong and J. E. Marsden. Lie-Poisson Hamilton-Jacobi theory and Lie-Poisson integrators. *Phys. Lett. A*, 133(3):134–139, 1988.